Project Number: NAG-0702

INTEGRATION OF A SMALL VACUUM FACILITY

A Major Qualifying Project Report:

Submitted to the Faculty

Of the

WORCESTER POLYTECHNIC INSTITUTE

In partial fulfillment of the requirements for the

Degree of Bachelor of Science

by

_____

Victor Herrera

_____

Michael Macri

_____

Von Tourgee

Date: February 2008

Approved by,

_____

Professor Nikolaos A. Gatsonis, MQP Advisor
Mechanical Engineering Department, WPI

Abstract

This project involves the integration of a bell-jar vacuum chamber with a microflow delivery system. A structure to support the bell-jar and associated equipment is designed for a 405 kg maximum load . A hoist mechanism is designed to allow lifting of the 114 kg bell-jar cover. The design and structural analysis of these systems are performed using software. This project provides also analysis and estimates of the mass flow that will be delivered into the bell-jar using a pressure-decay microflow system.

Acknowledgements

The MQP team would like to extend our sincere gratitude to:

Professor Nikolaos Gatsonis, Ph.D.
For his guidance, support, and motivation during the development and completion of the project.

Wael Ghazi Al-Kouz, Ph.D. candidate
For his advice and accurate help during the development of the project.

Authorship

Chapter 1: Introduction .....

Writing……Victor, Michael

Chapter 2: Design of Bell Jar Table .....

Writing……Michael

Technical……Victor, Von, Michael

Chapter 3: Hoist .....

Writing……Von

Technical……Victor, Von, Michael

Chapter 4: Fluid Mechanics……..

Writing……..Michael

Technical……Victor, Von, Michael

Chapter 5: Conclusions .....

Writing……Von

Appendix A: Matlab Code ..... Heller et al. (MQP 2006)

Appendix B .....

PRINCIPAL STRESSES ..... Victor

VON MISES CRITERION …… Victor

Table of Contents

Table of Figures

1. Introduction

Microfluidic and nanofluidic devices find applications in areas such as micro-propulsion, MEMS, medical diagnostics, genetic sequencing, chemistry production, life sciences. (Graveson et al 1993). The fluid mechanics associated with these scales is a subject of intense research (Karniadakis et al, 2007) and is pursued with theoretical, computational and experimental investigations.

A specific area in microfluidics is the study of gases through microchannels (Chamberlin and Gatsonis 2007). An important non-dimensional number characterizing microflows is the Knudsen number defined as the ratio of the characteristic length to the mean-free path for collisions between the gas species

$$Kn = \frac{\lambda}{D}$$

Depending on the diameter of the channel (D) and the incoming flow conditions flows in microchannels can fall in to the continuum, slip, transitional, and rarefied regimes.

Free Molecular: $Kn > 10$

Transitional: $10 > Kn > 1$

Slip: $1 > Kn > .01$

Continuum: $Kn \ll .01$

The goal of this project is to design an experimental setup and establish a Small Vacuum Chamber facility (SVaC) that will allow the experimental investigation of gaseous flows and jets in a wide regime of Knudsen numbers.

1.1 Review

Microfluidic experiments are challenging due to the scales involved. Specialized techniques and equipment setups are needed to register resulting pressures and flow rates. This becomes even more difficult when simple disturbances can become greater than the pressures that are to be measured. Microfluidics research at WPI involves experiments and computations and focuses on study of microchannel and microjet flows.

A previous MQP (LaPointe et al., 2005) initially designed an experimental setup for the investigation of micro-jets. This setup included a pressurized gas tank, pressure regulators, a filter, a mass-flow measuring tank, and a micro-nozzle. This setup is the original pressure decay method for mass flow. Later incarnations of this system rely on these initial calculations. The mass flow measuring tank is connected to the pressure transducer and separated from the reservoir and the vacuum chamber by control valves. The mass flow tank is then slowly discharged into the chamber at a mass flow rate proportional to the pressure decay rate in the control tank. The throat, leading into the chamber, having a diameter as small as 10 micrometers, is used as a nozzle.

The MQP by Heller et al. (2006) focused on the design of a flow system that can be used to study micro-jets and their effects on flexible structures. The goal of this project was to investigate the performance of micro thrusters that required measurements of very small mass flow rates down to 10^{-13} kg/s. No commercial flow meters for the nanoscale flows exist. In order to get mass flow rates at this level, an alternative method is needed. The pressure decay method, works by using two reservoirs, a main tank and a secondary tank. This method uses the constant volume of the secondary tank and the pressure to allow for mass flow rate to be calculated using the ideal gas law. The main tank is a high pressure tank, that is used to fill the secondary tank which is then isolated from the system using pin valves. The downstream valve is then opened, and an ionization gage pressure transducer registers pressure loss. From this pressure drop a LabVIEW Virtual Instrument can be setup to calculate mass flow. (Heller et al 2006)

Two reports by Chamberlin and Gatsonis (2006) deal with the Direct Simulation Monte Carlo Method (DSMC), which is a numerical approach used for flows in microtubes. In Chamberlin and Gatsonis (2006a) the expansion of argon jets from cylindrical microtubes is investigated; it was found that the plume shape is shown to narrow with increasing Knudsen number, increasing aspect ratio, and decreasing Reynolds number. In Chamberlin and Gatsonis (2006b) the expansion of nitrogen from a microjet into vacuum using the DSMC code in order to design a micropitot tube. The simulations predicted pressure range of 100 to 0.005 Pa to be the required operating range of the micropitot probe pressure sensor. Figure 1 is a schematic of this experiment.

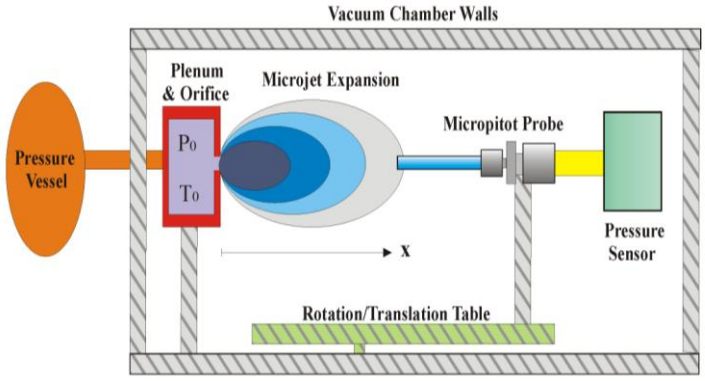

Figure 1 Experiment Setup from Chamberlin and Gatsonis (2006b)

The goal of this project is to design a Small Vacuum Chamber facility (SVaC) shown schematically in Figure 2. The SVaC allows for experiments that simulate high atmosphere conditions and low background pressures. The SVaC consists of the bell jar, the base well, the hoist system the vacuum pump and the support structure.

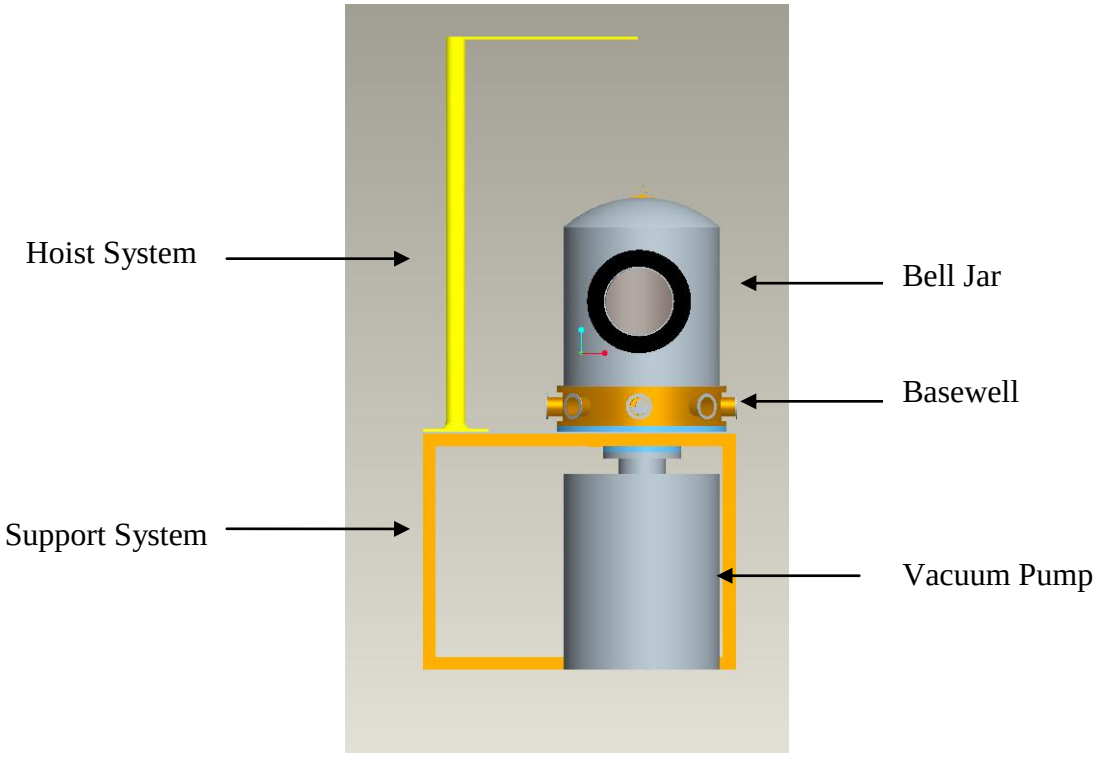

Figure 2 Bell Jar and Support System

The Bell Jar (Ref#SSBJ-24) to be used is manufactured by MDC, a vacuum products company. It has a 24" diameter, and a 30' height. It has a feed through Base well (FTCO-K150-24) attached on the bottom with the same diameter and 6" height; the purpose of this Base well (BW-K150-24) is to provide inlets for cables that go into the experiment and connect the Bell Jar to the Vacuum Pump. It also has a 6" glass viewport for experiment observation. The weights of the Bell Jar and base well are 250 lbf and 237 lbf, for a total of 487 lbf.

1.2 Objectives and Approach

The design objectives, design requirements and approach are outlined in this section.

1.2.1 Design of a Support Structure for the Bell Jar

Requirements

- A Support Structure (table) that can hold 750 lbf is required. This weight includes the Bell Jar, its equipment, and a possible Hoist System attached to the table.
- The table should have a safety factor of 2 in terms of yield stress and it should not deflect much more than 1 mm.
- The support structure must be in 100 lbf-300 lbf due to load and pressure concerns on the floor.
- The surface area of the support structure must be large enough to accommodate the 24" inch diameter Bell Jar and a Hoist System.
- The surface area must have a 12" hole to accommodate the Base well.
- It must be tall enough to accommodate the Vacuum Pump underneath it.

Approach

The support structure is designed using the solid modeling software ProE. The structural capabilities will be tested under the required loads using with ProMechanica. Several iterations under various design configurations are explored until a satisfactory configuration is reached.

1.2.2 Design of Hoist System

Requirements

- A Hoist System (Figure 1) is required to lift the 250 lbf Bell Jar cover from the Base well and clear its 30" height.
- The Hoist System must not be taller than the ceiling height, 13 ft.
- The Hoist System can either be free standing or mounted on the support structure, both iterations were tried.
- It can either be electrical or mechanical.
- The Hoist system must also be able to move the Bell Jar away from the Base well center axis, so it will not be directly above it when lifted due to safety reasons.

Approach

Investigate available free-standing and attached Hoist Systems and integrate with the Support Structure, Perform structural analysis using ProMechanica.

Design a free-standing Hoist System using ProE. Perform structural analysis using ProMechanica of a custom designed free-standing Hoist System.

1.2.3 Computational Fluid Dynamics Simulations

Requirements

- There will be two tube sizes considered for the simulations, 10 micron and 100 micron.
- Nitrogen gas will be used with pressure ranges as follows:
    - 10 micron pressure for continuum flow is greater than 53,210 Pa
    - 100 micron pressure for continuum flow is 5,321 Pa
- Due to software limitations only contiuum flow may be modeled.

Aproach

Micro tubes were designed and meshed using Gambit, they were given pressure based inlets and outlets and run in FLUENT. Velocity Fields were generated to verify a correct run and pressure results were also produced.

2. Table Design and Analysis

A table is needed to position the bell jar in such a way that the pump can be mounted and the chamber top is available to access. The flow system must also be close to the chamber for ease of access. Pro-Mechanica was used to test a suitable table design and ensure it would not fail under the weight of the test equipment.

2.2 Design Requirements

The chamber is 1.02m (40”) tall and is 66.04cm (26”) outer diameter. The chamber weighs 500lbs and has its pump port located on its underside. The pump port flange is the widest section that will have to pass through the hole being 279.4mm (11in) wide. With this in mind a list of design constraints was produced. The bell jar dimensions are shown in figure 3.

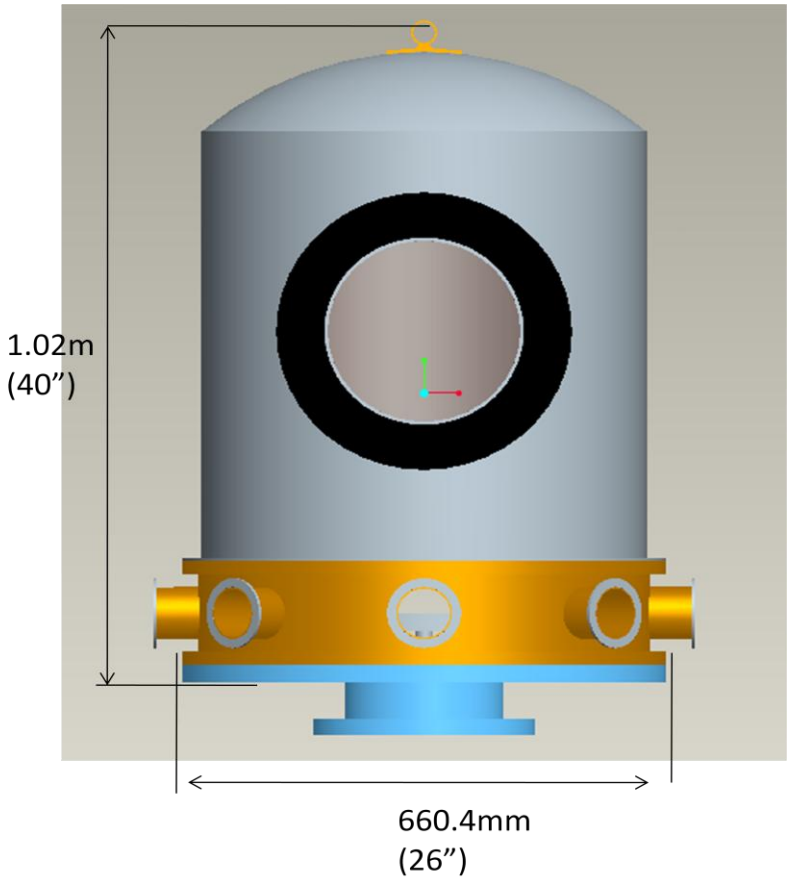

Figure 3 the bell jar size

The table must have hole through the top large enough to allow the pump port to fit through and connect to the gate valve below the table. The hole diameter was chosen to be 304.8mm (12in) to allow for an easy drop in for the base well. Two different setups for the table hole placement were tested, one with the hole centered and one with it offset to one side.

The table must be of sufficient strength to support the weight of the chamber and the pump and gate valve. A test weight of 3336.2 N (750lbf) was chosen to model this weight as the pump weight is still unknown; however, this weight is more than the expected combined weight of the system which would be about 2668.9N (600lbf) to provide a factor of safety. Steel was determined to be the best choice for the construction material A36 for the table top and A500 for the frame. Both of these have a young's modulus of 2.01×10^{11}Pa (4.177×10^{9}psf). A36 has a yield strength of 2.482×10^{8} Pa (5.184×10^{6} Psf) and an ultimate tensile strength of 3.833×10^{6} Pa (8.0064×10^{6} psf). A500 has a yield strength of 2.896×10^{8} Pa (6.048×10^{6} Psf) and an ultimate tensile strength of 2.944×10^{9} Pa (6.148×10^{7} Psf). For the sake of easier movement a maximum unloaded table weight of 250lbs was set.

Several Constraints were also placed on the shape of the table. The table must be tall enough to accommodate a pump. The underside of the table must allow for the pumps to be slid under it and easily aligned for installation. To facilitate this it was decided that if lower horizontal support were used they would only be used on 3 sides the same was decided for a design with more than four legs.

With these requirements in place, design iterations were drawn in Pro Engineer and tested in Pro Mechanica.

2.3 Modeling

Each design iteration was designed in Pro Engineer and analyzed with Pro Mechanica. The procedure for modeling these iteration is described in detail in this section. First the model is built in Pro Engineer component by component in separate .prt files. These separate parts are then combined in an assembly. Pro Mechanica has a weld and a fastener feature, but as the models do not call for bolt fasteners, and welds are stronger than the actual parts they connect, the components were mated together. This could be done because the frame pieces are thin

enough for a fully penetrating weld, and the table top rests on the frame in such a way that the weld simply keeps it in place and does not bear a significant load.

Once the table was assembled, the material properties described in the above sections were applied to the different components of the model. As the table rests on the ground, displacement constraints were applied to the bottom of the table frame. Densities were assigned to the materials and a gravity load of 1 G was applied in the negative z direction. Finally the load of the bell jar was distributed along a (26in) diameter region minus the (12in) hole. This completed the preliminary modeling.

Pro Mechanica uses finite element analysis to calculate internal stresses throughout the model. Unfortunately, the program was unable to provide us with reaction forces on the floor as a result of the table load. This is likely due to Pro Mechanica being designed primarily for mechanisms.

2.4 Design Iterations

The first design iteration was simply a solid 101.6mm (4in) thick steel plate. The purpose of this was to determine whether the required hole would compromise the table's structural integrity. At this point 2 options were considered. The first option was for a centered hole for ease of calculations, the second was for an offset hole, this was proposed to move the chamber closer to the supports and allocate space for the flow system. After testing it was found that the offset option and the centered option differed only slightly and the offset option was set as the primary design.

The fame was then added to the table and the original 101.6mm (4in) thick piece of steel was reduced to 4.72mm (3/16in) thick and a steel box frame was added to the complete the model. The box frame was 4.72mm (3/16in) thick and was 50.8mm (2in) square cross section. The Table top and frame are shown in figure 4.

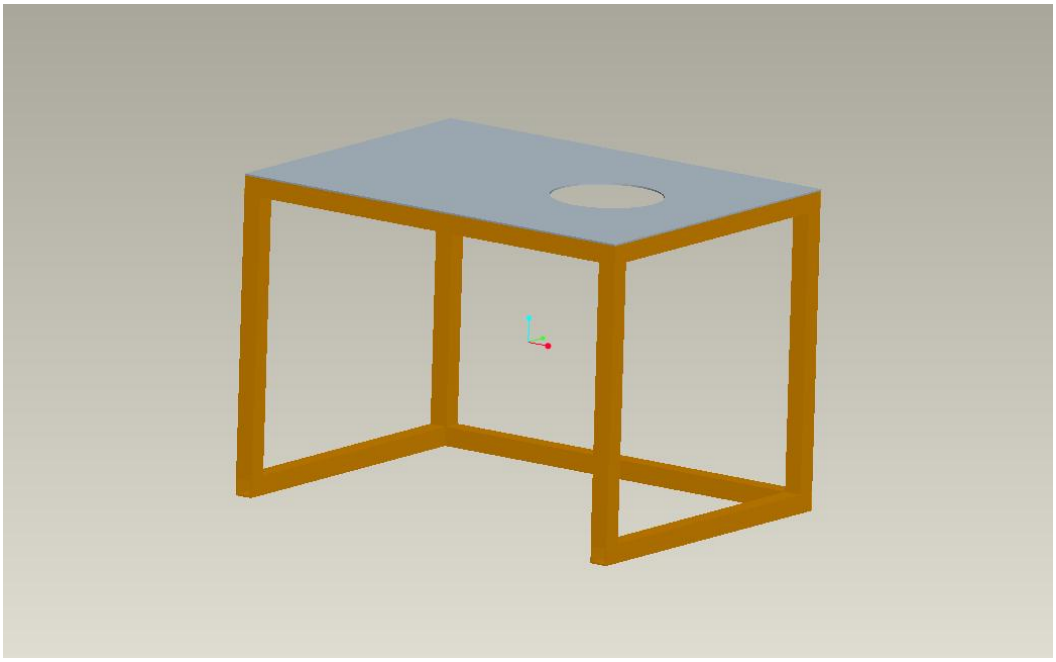

Figure 4 the table top and frame assembled in Pro Engineer

Once this initial design was completed Pro Mechanica testing commenced. Displacement constraints were placed on the bottom of the fame to simulate a floor beneath the table and a load was applied to the contact area where the Bell Jar would be supported. The load of 750 lbs was applied uniformly to a contact region with an outer diameter of 660.4mm (26in) and an inner diameter of 304.8mm (12in). A gravity load of -9.8m/s^2 (-32ft/s^2) was applied in the z direction. Once the loads and the constraints were in place Pro Mechanica's structural analysis tool was used to generate graphic fringe charts to show the location a magnitude of various physical properties which were then compared to the failure criteria stated in the above section. The loaded table is shown in the figure 5.

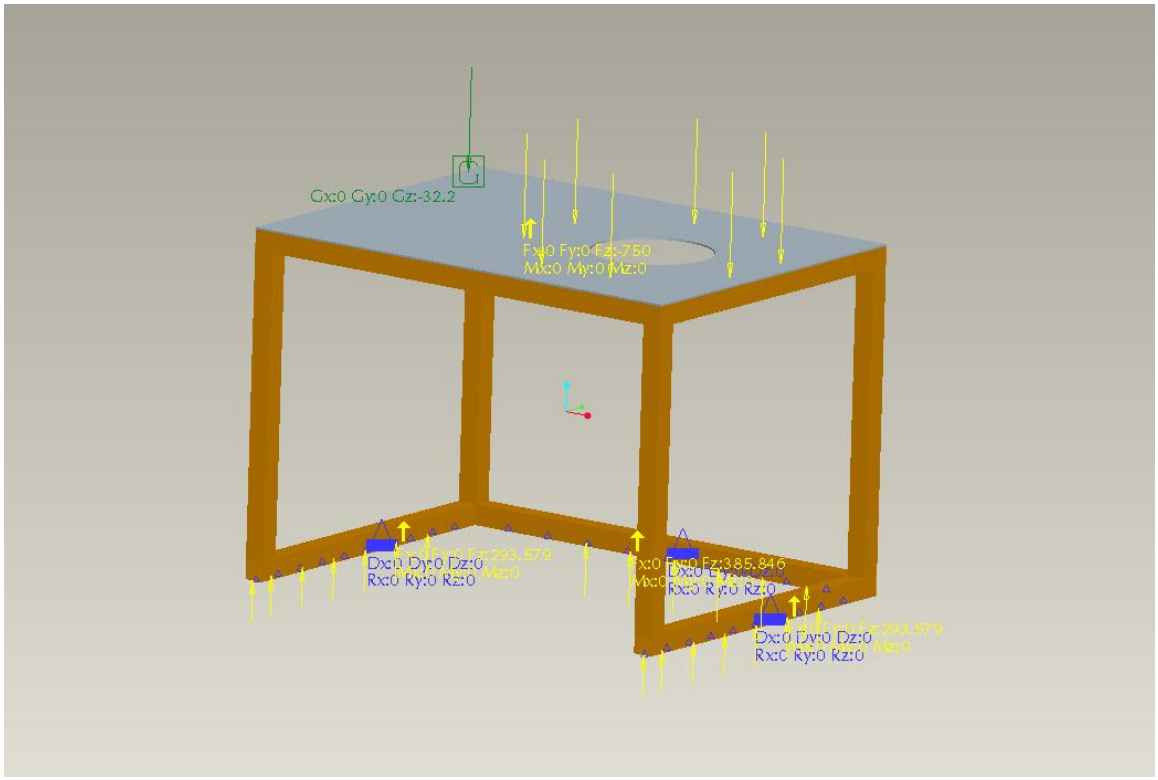

Figure 5 the table loaded for the analysis

Pro Mechanica uses a Finite Element package to perform structural analysis results for Max Principle Stresses and Maximum Von Misses Stresses were generated[1]. The Von Misses results are shown in figure 6, and the Max Principle stresses are shown in figure 7 The largest Von Misses and Max Principle Stress were below the failure criteria set above.

[1] For a detailed description of Max Principle and Von Misses Stresses please refer to Appendix B

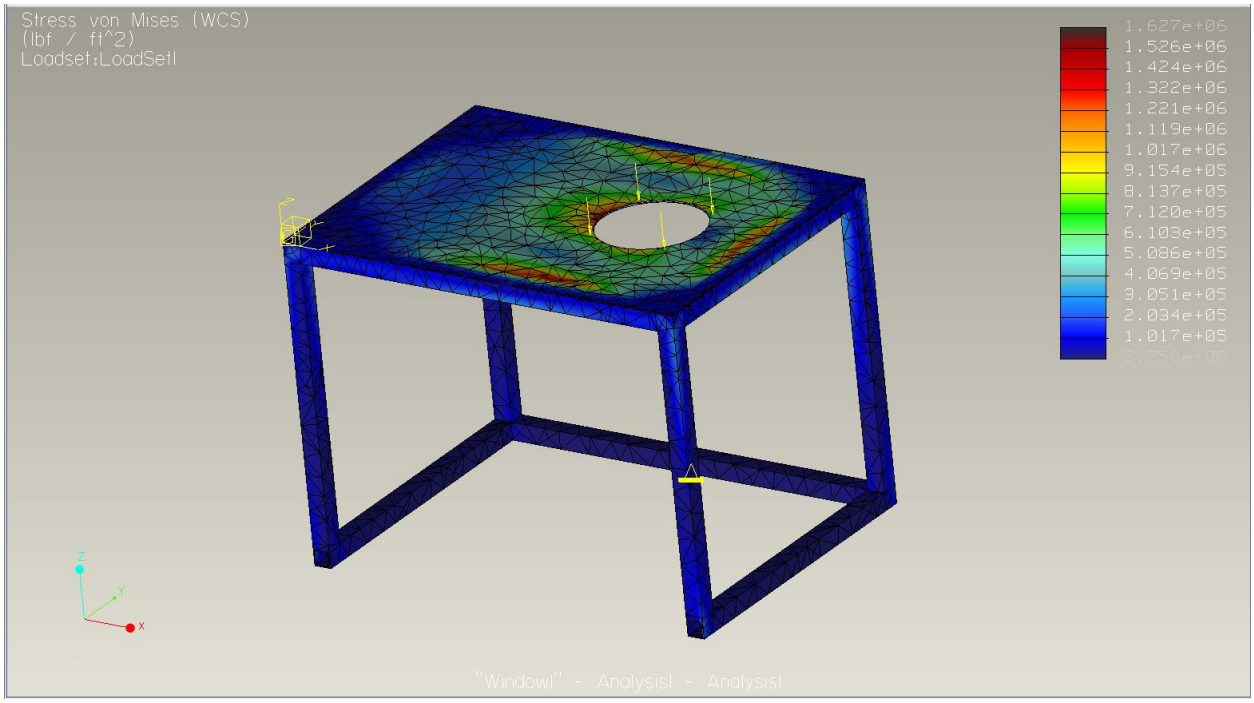

Figure 6 the Von Misses Results for the offset hole table

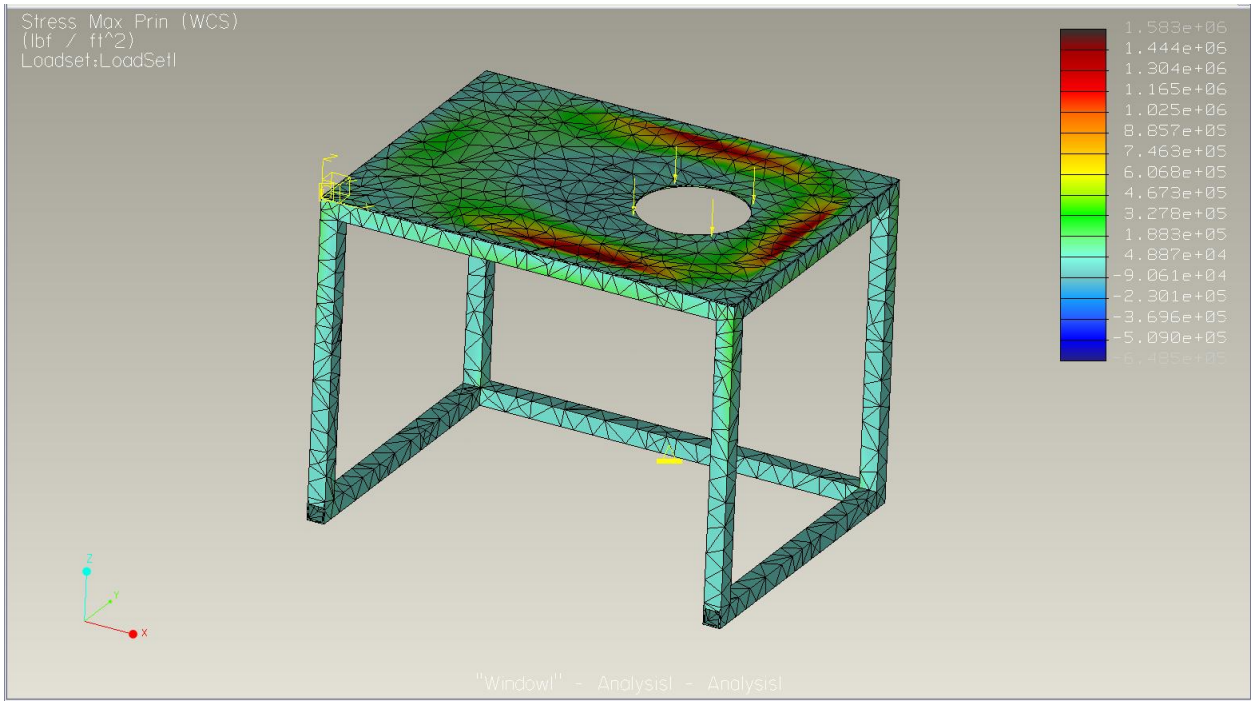

Figure 7 the Maximum Principle Stress

From the results it was determined that the table could support the load, but the displacement results were out of the original design specifications being over 3mm as shown in figure 8.

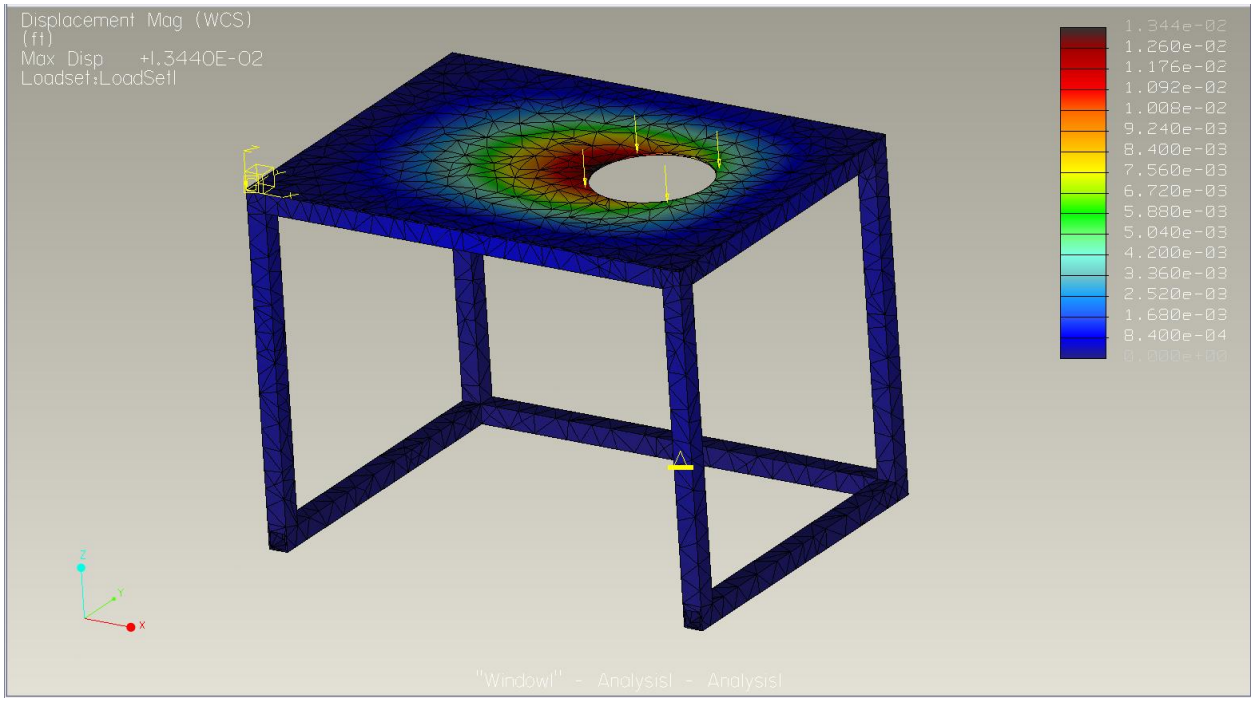

Figure 8 the Displacement Results (.01344ft=4.09mm)

To rectify this, a support bar was added to the underside of the table across the center to provide additional support for the table top. This bar had the same geometry as the original frame. The analysis was run again, with the modification the displacement results fell into specifications as indicated in figure 9.

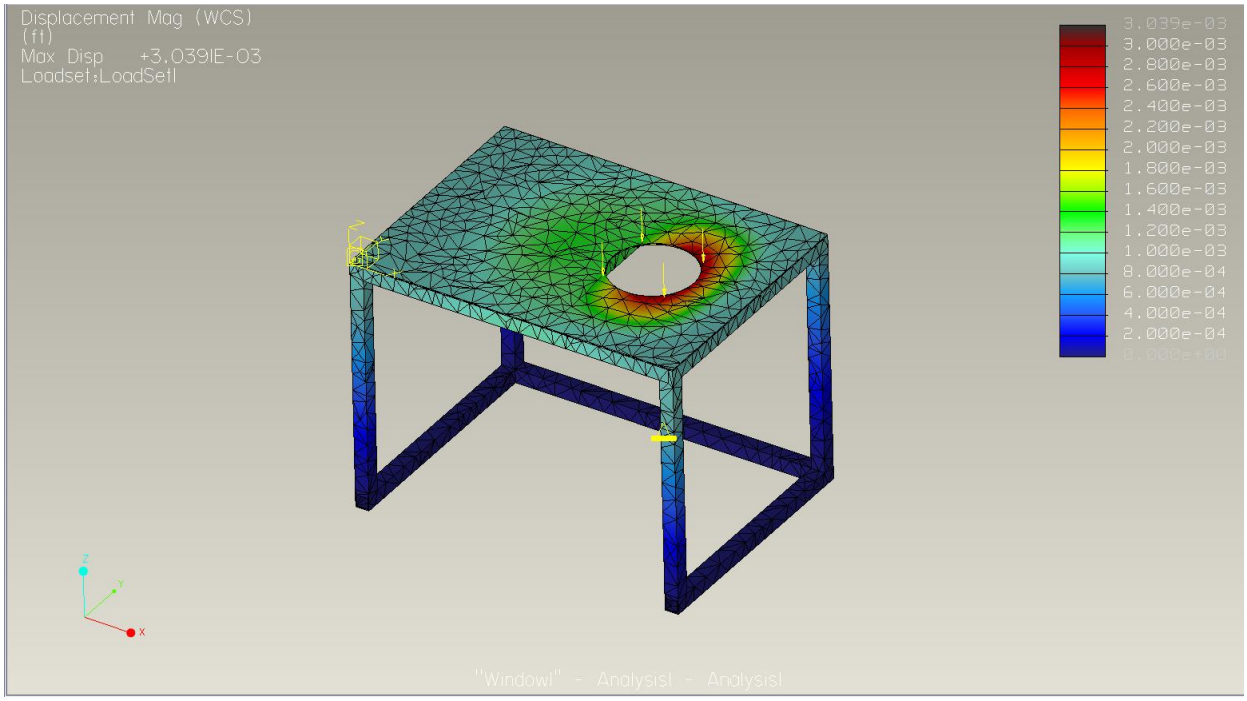

Figure 9 the displacement results after the cross beam was added (.003ft=.914mm)

The final table meets all design requirements set in section one of this chapter. The overall weight of the table was 1040.88N (234lbf) unloaded and 4378N (985lbf) fully loaded.

3. Design of a Hoist

In this chapter the hoisting mechanism is introduced. The design process for the hoisting mechanism was filled with many creative designs, with much iteration, and unique avenues explored. The design requirements were very specific in what needed to be accomplished and at the same time very open ended when it came to how the task should be attacked. The design team began with preliminary research into the industrial hoist field. Once a firm grasp of the existing hoisting mechanisms had been achieved the design team began with brainstorming sessions which lead them to the first iteration, the free standing gantry crane. The gantry crane was deemed too expensive which lead to the second iteration which involved incorporating the gantry crane design into the design of the table this second order iteration is referred to as the attached gantry crane. The attached gantry crane became too tall and weighed too much to be practical. The third order iteration involved the retrofitting of a free standing cantilever crane combined with an I-beam this design deflected an unacceptable amount and was not pursued. The fourth and final iteration is the Vestil crane named after its manufacturer, this crane is light weight, easy to incorporate into our table, and is inexpensive. The Vestil crane is incorporated into our table and a Pro Mechanica design study has been conducted to confirm that all forces exerted onto the table, and lifting mechanism are acceptable.

3.1 Design Requirements

To perform the experiments, it is necessary that the operator has access to the inside of the chamber. The bell jar weighs 113.4Kg (250lbs). This load cannot be lifted safely by a single operator, which is why a hoisting mechanism is required. The design requirements include the following. The hoist must be able to lift 113.4Kg (250lb) safely. The hoist is to be designed so that a single operator can maneuver the bell jar into and out of its operating position. It must be able to move the bell jar up 34 inches to achieve complete clearance of the volume which it contains during operation. This will allow the instruments in the experiments to utilize the full volume that the bell jar can offer. The hoist needs to be able to move the bell jar away from the collar while at its maximum height. This is required to allow the operator to work on instruments in the staging area without having a 113.4Kg (250lb) bell jar hanging over them. The hoist is to be integrated into the table (which is show in figure 10) which will hold the bell

jar, and experimental instruments. Cost as well as weight must be kept to a minimum in the design of the hoisting mechanism.

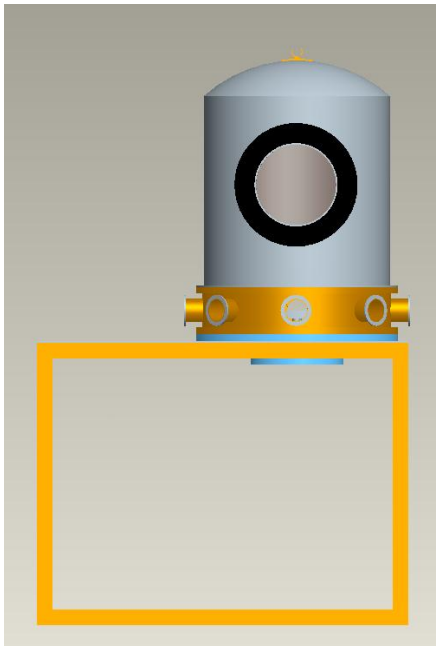

Figure 10 Bell Jar and Table

3.2 Preliminary Research

The first step in the design process was research. There are a lot of different ways to lift this load, it is important to find the most practical, cost effective, and easiest for the operator to use. It took several iterations to come to the best solutions to this problem. The problem was broken into two parts. The first being the vertical lift and the second being the planer movement away from the staging area, once the bell jar is lifted. There were many initial ideas about how to lift the bell jar. Several members of the team through their experiences in construction believed a simple "come along", or electrical winch (see figures 11 and 12) would be appropriate.

Figure 11 The Manual Hoist

Figure 12 the Electric Power Hoist

Based on the knowledge that with either of these two options an operator will be able to lift the bell jar by him/her self work began on the planer movement of the bell jar.

3.3 Free Standing Gantry Crane

Again there are several options which need to be considered to fulfill this requirement for the design. Some of the preliminary ideas include the use of a portable gantry crane (see figure 13), and trolley combination (see figure 14).

Figure 13 A Portable Gantry Crane (This image illustrates the idea of an I-Beam trolley crane)

Figure 14 I-Beam Trolley

The trolley will be connected to the I-Beam section of the gantry crane and then the "come along" or electric winch will be connected to the trolley. The end of the winch or come along will then be connected to the bell jar. The winch or come along will lift the bell jar to the desired height, and once lifted the operator can push the bell jar along the length of the I-Beam via the trolley. The device would have worked well except that it had an unacceptably large price tag. The gantry crane alone has a minimum cost of 900 dollars. Another subset of this

iteration is the possibility of using just the trolley and electric winch or “come along” when it came to our attention that there are exposed I-beams in the room where the vacuum apparatus will be housed. This notion is abandoned because it is not known if the I-Beam could handle the load of the bell jar and also because the I-Beam is on an angle. Motorized trolleys are investigated as a possible solution; however, it is not known if the wheels will have a large enough coefficient of friction to be able to move the bell jar without slipping.

3.4 Attached Gantry Crane

The next logical step which is taken is to try and incorporate the basic idea of a gantry crane into the design of our table to try and drive down the price of the hoisting unit. It is believed that by incorporating the two the cost issue will be alleviated by manufacturing the device in house. The system which is first considered consisted of two long vertical bars and two small bars on top of the two previous ones placed perpendicular to them. These two bars will hold an I-Beam which will support a trolley with a hoist lift please refer to figure 15. All the bars that hold the hoist mechanism are modeled as 3/16” wall thickness rectangular tubing.

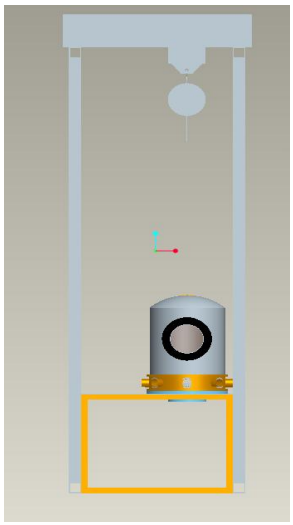

Figure 15 Incorporated Gantry Crane

It is known that the I-Beam could handle this load via information from the manufacturer so a stress analysis is not necessary. A stress simulation is necessary for the supporting frames which hold the I-Beam in place. The factor of safety is set at 2 so the stress simulation is run with a weight of 227.3kg (500lbs). In figure 16 and 17 the majority of the stress is concentrated

at the center of the frame's top cross member; however, it is important to note that the structural integrity of the frame is intact, and it can safely support the load with the factor of safety set at 2.

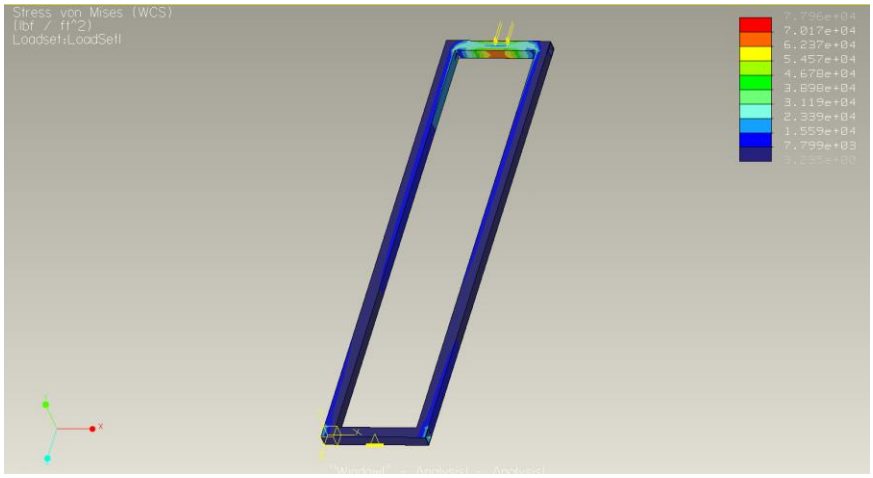

Figure 16 Von Misses

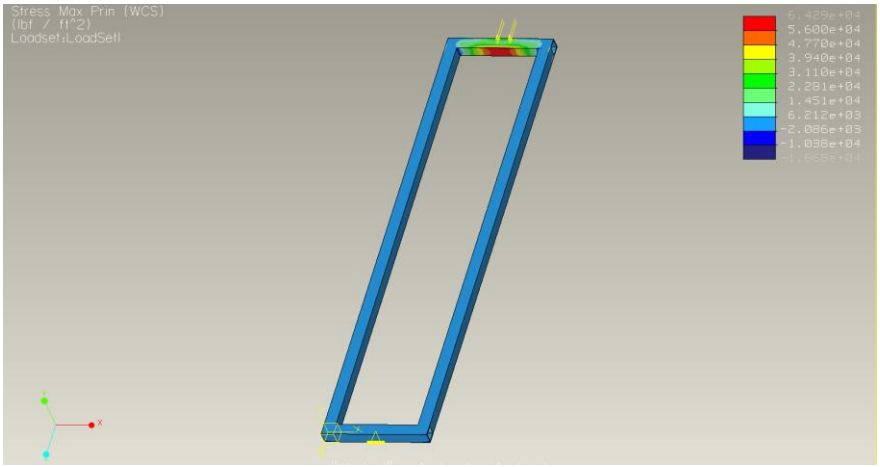

Figure 17 Max Principal

Two issues arose with the integrated gantry crane hoisting system. The first problem with this iteration is that it was too tall to fit in the room which is available to house our vacuum chamber. With the table already at 4 feet tall and the electric winch 2 feet long at its shortest, add in the I-Beam, trolley, and collar and the system becomes too cumbersome and tall to be practical. At this point that the design still has some promise. If different components are selected, and some minor modifications are made it is thought that this basic design still has validity. These premature notions are derailed once the weight of the system is taken into account. The design is

too large to be practical and at this point no further effort is wasted trying to make it work. It is clear that another direction must be explored.

3.5 Free Standing Cantilever

The next iteration is a freestanding cantilever beam modified with lower support bar as opposed to a tension rod frame which will be a combination of figure 18 and 19. The modification is necessary to lower the total height of hoisting mechanism, while still allowing the hoist to raise the bell jar by the required 34 inches.

Figure 18 this structure could be modified so that the tension rod is not needed

The tension rod support can be replaced by running a beam parallel to the vertical support similar to the wall mount shown below.

Figure 19 (this can be welded to the vertical support minus the hinges instead of the tension rod)

Using this hybrid will meet the requirements of the hoisting mechanism. It will operate much like a gantry crane using a trolley and winch combination to achieve the movement of the bell jar needed. The system is less expensive than the gantry crane system but is still on the expensive side. This expense comes from the fact that an electric winch is needed because trying to use a

manual system will not work on account of the height at which it will have to be operated at. The operator will not be able to reach the handle of a manual system safely. Again to try and drive down the price the design team ran an analysis of a system which is to be built rather then ordered. The free-standing hoist model is analyzed. This design consists of three-bar base, two vertical bars attached to each other, and a horizontal I-Beam resting on top of the vertical bars. This model has the benefits of using less material and occupying less space. Figure 20 represents the model and the table.

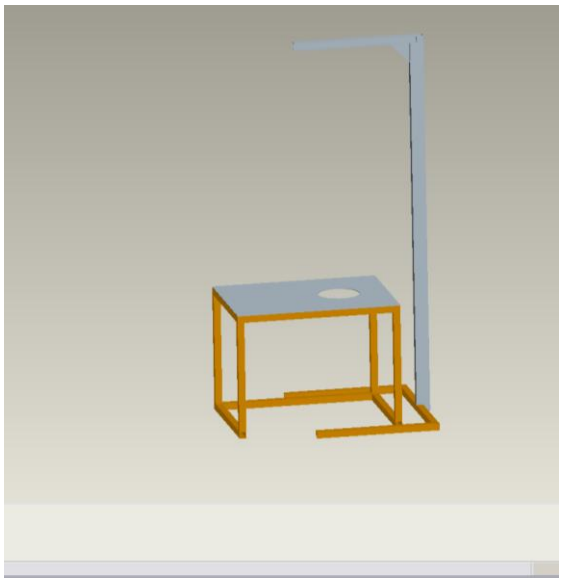

Figure 20: Cantilever Hoist

An FEM analysis is performed on this hoist model to ensure that the stresses are less than the yield stress allowed for A500 steel and that the displacement is negligible. A force of 350 lb is placed on figures 21, 22, 23 which represent the Von Mises stress, the Maximum Principal stress and the displacement on this system.

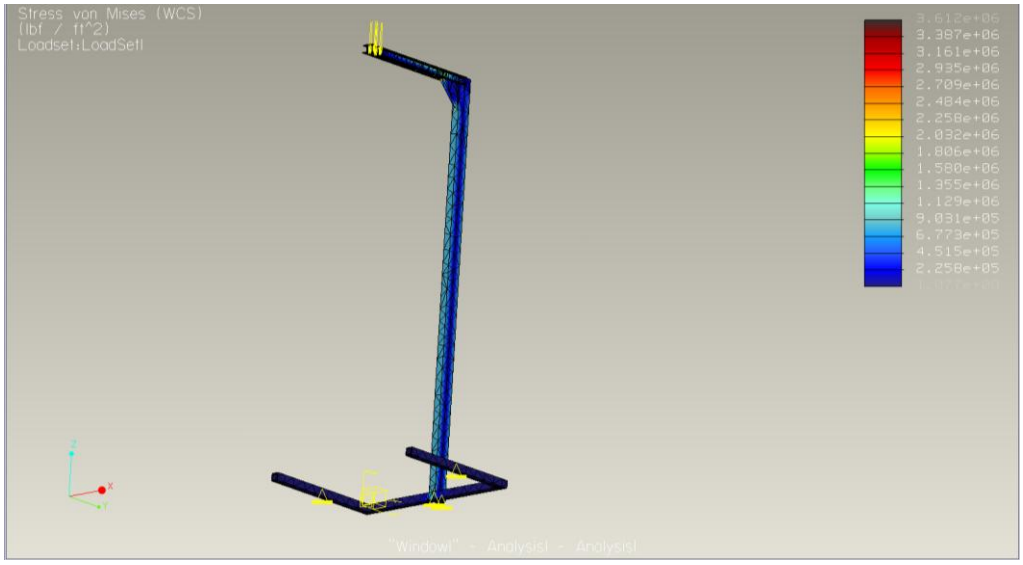

Figure 21 Von Mises

Figure 22 Maximum Principal

Figure 23 Displacement

The stresses are bellow the yield stress for A500, giving an approximate factor of safety of 2. However, the max displacement is approximately 20 mm. This is more than desired and for this reason this option is not considered.

3.6 Vestil Crane

Another option which up to this point has not been explored again, involved retrofitting an existing design which is not meant for this purpose. The basis for this hoisting system is a pickup truck crane. The crane was originally designed to be bolted down to the bed of a pickup truck and then depending on the boom angle, and how far out the telescopic boom is operating at could lift from 227.3kgs (500 lbs) to 454.5kgs (1000lbs). The crane is shown in figure 24.

Figure 24 Vestil Truck Crane

There are several capabilities this crane has which make it a prime candidate for the job at hand. The first is that the crane can pivot 360° this ability is useful if for whatever reason the bell jar needs to be completely removed from the table it is resting on. Also this conveniently solves the issue of planner motion once the bell jar is at height. The boom moves up to an angle of 60°, and is telescoping which when not in use will not be in the way of the operator. Another attribute which made this model crane an attractive choice is its low price tag. This model is approximately one half to one third the price of the other options which had been considered. The savings came at the price of having a manual crank rather than an electric winch. This will not be an issue anymore because the crank is located relatively low on the model and will be safely accessible to the operator. In addition to the low cost the crane is incredibly light coming in at 64.1kg (141 lb).

The table which was already designed at this point has to be modified so that the crane can be integrated properly. The base of the crane will be placed in the far corner from where the bell jar will be resting during operation this will keep the crane out of the operators way as much as possible. An additional sub structure made from the same square tubing used on the rest of the tables frame has been added to help support the crane when in operation. The model has been simulated using Pro Mechanica with the stress results shown in chapter 3.7

3.7 Pro Mechanica Design Study

. To determine what effect the hoist will have on the table a Pro Mechanica design study was conducted. The stresses acting on the crane itself will not be taken into consideration because the manufacturer already set the safe operating conditions for the crane which will not be exceeded. Therefore a safe assumption is that the crane is a solid rigid body. Of more concern is the effect the forces from the base plate of the crane will enact onto the table. It is necessary to make sure these stresses are in the acceptable range. The team ran into difficulties with Pro Mechanica's fastener feature and moment load features. As a result a simplified analysis is used. The resultant loads that will be generated by the bell jar suspended from the boom is calculated as 2 distributed loads one on the left and one on the right, for 2 different configurations. The first is with the crane extended in the x direction (the long way) and the second with the boom in the y direction (the shorter direction). The results are shown in figures 26, 27, 28, and 29 which are within acceptable limits. For figure 25 (configuration 1) the right section is loaded with (257lbf) and the left with (143lbf).

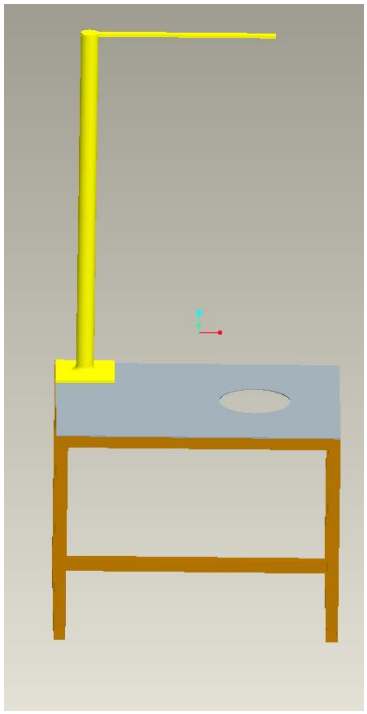

Figure 25 Configuration 1

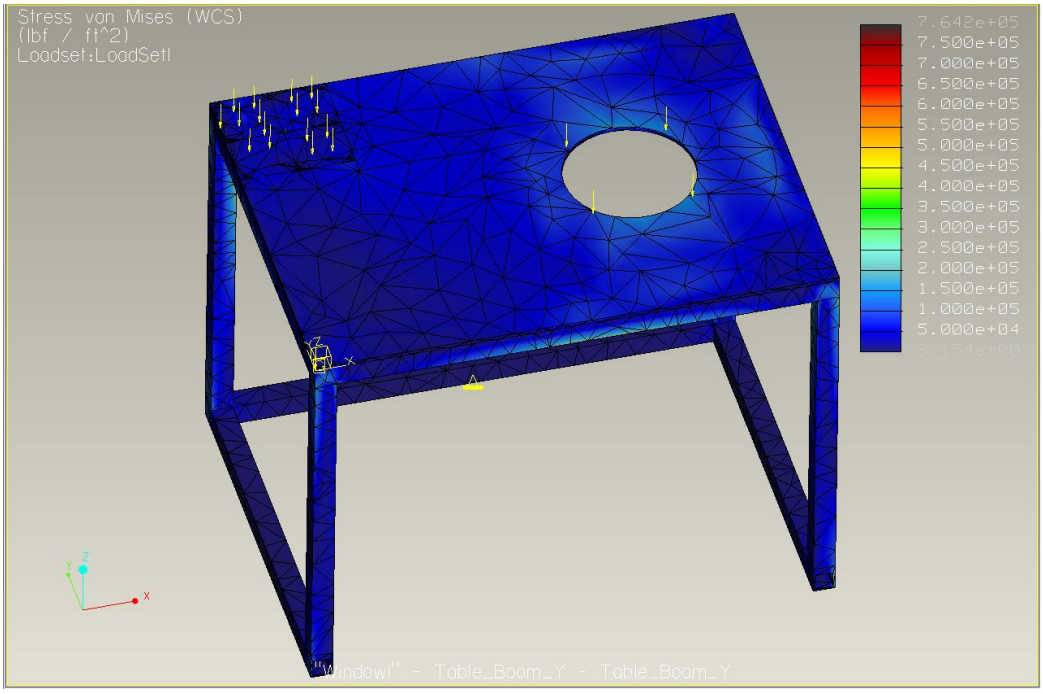

Figure 26 Von Mises results Max= 7.642e5 psf

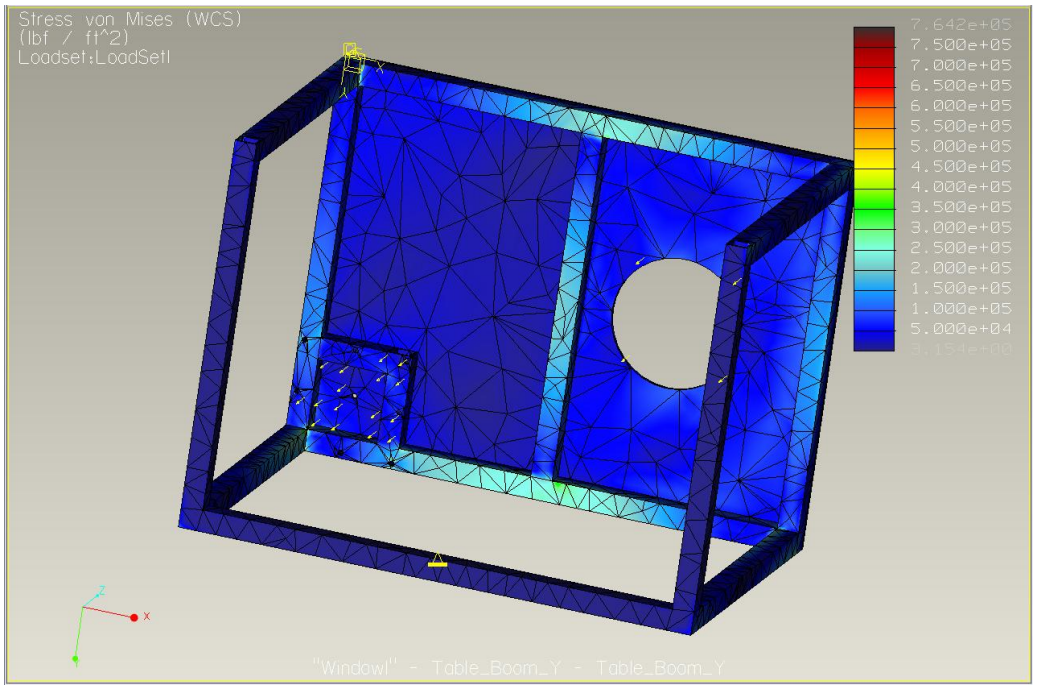

Figure 27 the bottom Von Mises view

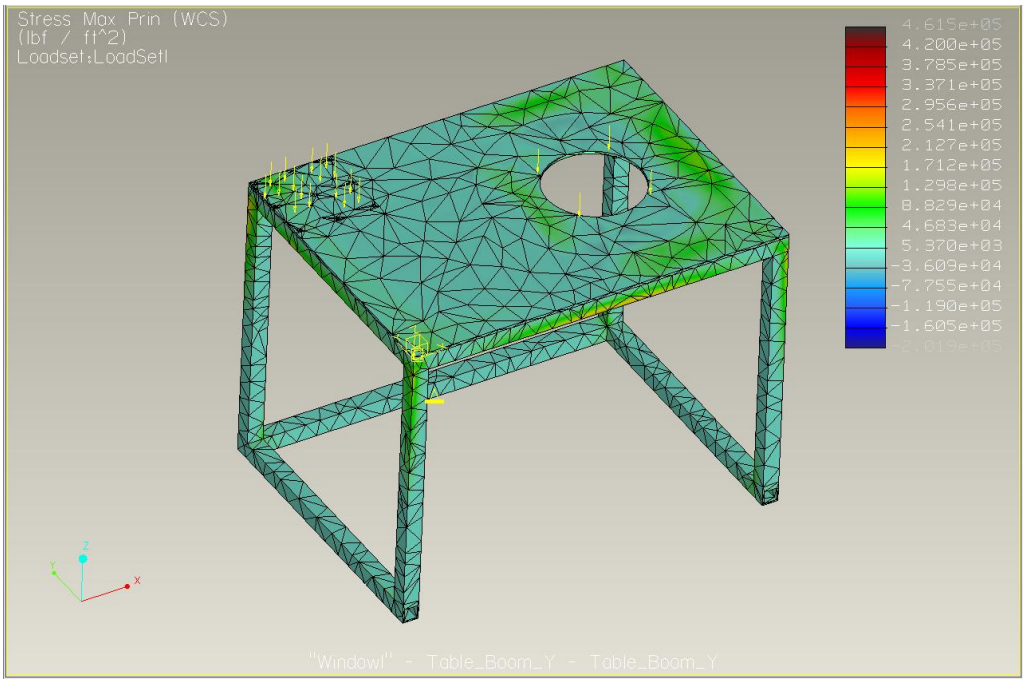

Figure 28 the Max Princ. Stress results Max= 4.615e5 psf

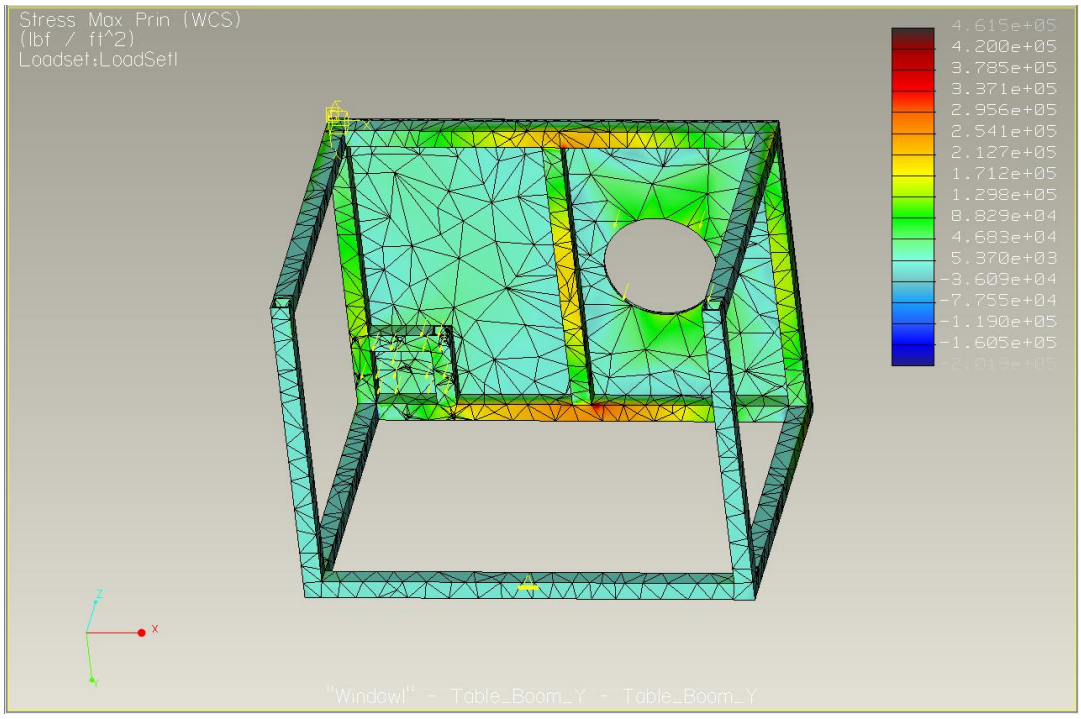

Figure 29 the bottom view of the max princ.

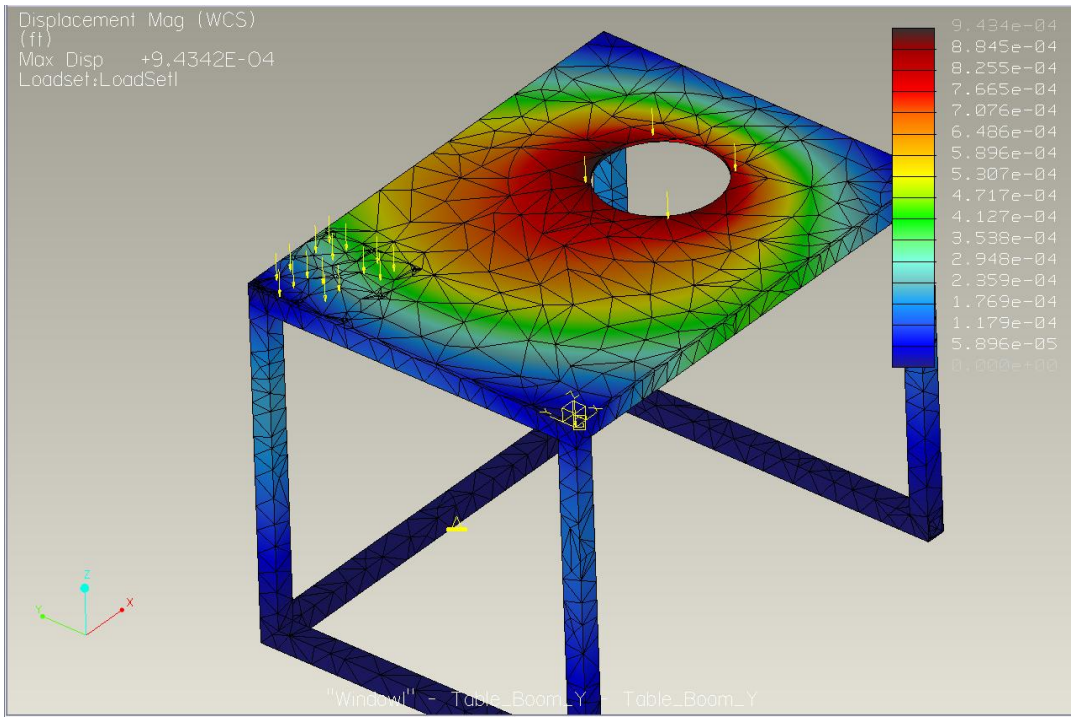

Figure 30 the Displacement Max=.28mm (9.4342e-4 ft)

Figure 31 configuration 2 is loaded with 2 contact areas top and bottom force, because the base is symmetrical the top was loaded with (134 lbf) and the bottom was loaded with (257 lbf).

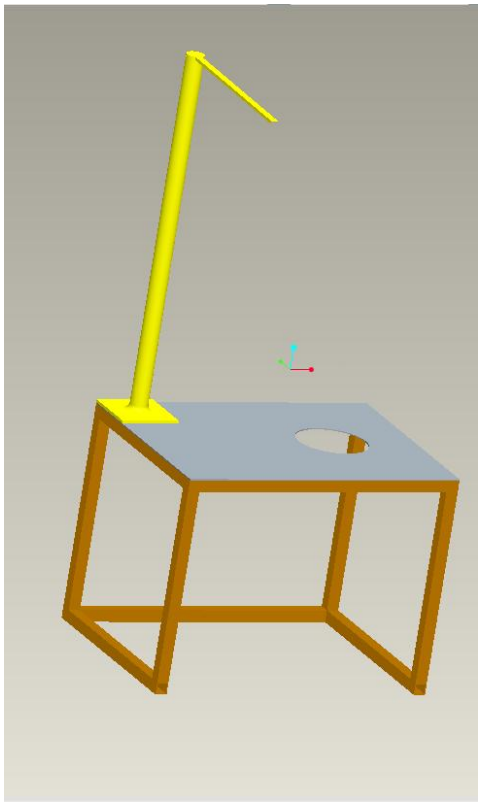

Figure 31 Configuration 2

After reviewing results, it was found that configuration 2 produced results that were similar to configuration 1, all the results are in the acceptibale range.

4. Analysis of Microflows

The reason for building this test chamber is to determine experimentally what the characteristics of the gas plumes are, and it is also to test the microscale pitot tube. To this end, FLUENT was used to simulate gas flows in microtubes. In order to run such simulations, information on the inlet conditions needed to be calculated and the chamber pressure would have to be set to an appropriate level. The simulation needed to be as close to the actual experimental conditions as possible. Using a modified version of the pressure-decay method code developed by Heller and Padden in their 2006 MQP was used to run a simulation with various inlet conditions. Upon achieving conditions that produced a near steady flow rates for an extended period of time, the simulations in FLUENT were run.

4.1 Flow Regimes and Knudsen Number Calculations

There are several different flow regimes within the scope of the testing that will occur. Continuum flow is the flow that most people are used to dealing with, it can be described by the Navier-Stokes equations, and follows assumptions such the no slip condition. Slip flow is the next level down in the regimes, it is similar to continuum in that it can be described with the Navier-Stokes equations, but it has a slip velocity at the wall that is not zero. Transitional flow is a complex regime that cannot be modeled accurately by any one equation; it is a combination of rarefied and continuum flow. The simulation code developed by Heller and Padden uses a combination of the Navier-Stokes and free molecular flow to model it. The lowest regime with which this experiment is concerned is the free molecular regime, here the gas has become fully rarefied and the equations actually track the individual molecules. The Knudsen number for the various flow regimes are shown in figure 32.

Free Molecular: $Kn > 10$

Transitional: $10 > Kn > 1$

Slip: $1 > Kn > .01$

Continuum: $Kn \ll .01$

Figure 32 The breakdown of Knudsen Number for various regimes

The formula for the Knudsen Number is the characteristic length, divided by the mean free path. For the purpose of this experiment the characteristic length is the diameter of the nozzle.

$$Kn = \frac{\lambda}{D}$$

The mean free path of a gas is a function of the molecular diameter (d) of the gas, its pressure (P), temperature (T), and the Boltzmann constant (k).

$$\lambda = \frac{kT}{\sqrt{2\pi} d^2 P}$$

The gas we chose for our simulations was Nitrogen, as it is the most likely candidate for the experimental gas, and it properties are very similar to air. It has the a molecular mass of 28 g/mol, a molecular diameter of 4.988e-10m, a specific gas constant of 296.8 J/(kg*K) and as a diatomic gas, has a ratio of specific heats equal to 1.4. Based on this information, and the target Knudsen numbers, pressure ranges were derived for various nozzle diameters. These ranges were used in the Matlab code, and ultimately the final FLUENT simulations.

4.2 Matlab Pressure Range Calculations

Once the pressure ranges for each flow regime was determined, the background pressure of the vacuum chamber had to be determined. Similarly simple physics tells us that the pressure inside the chamber must be lower than the reservoir pressure in order for there to be flow into the chamber. A further restriction was added that, because of its convenience of near constant flow rates, sonic flow at the nozzle would be preferred. The pressure ratio to maintain sonic flow is a pressure ratio of chamber pressure to reservoir pressure less than .528. A typical diffusion pump has an operating pressure of about .187Pa to 6.666e -7Pa, this is well below any of the calculated pressure ranges. This satisfied all of the above requirements.

The Matlab code was written to simply predict mass flow rate through an orifice with a reservoir pressure on one side and a chamber pressure on the other. From continuity, it is known that this mass flux will be constant anywhere downstream from the orifice. Using the Matlab code we checked our pressure ranges to verify that they produced flow in the correct regime, for a long enough time, and that the mass flow rate was consistent. This was done for all the 1, 10,

and 100 micron orifices, for nitrogen. Graphs were generated with the code and are shown in figures 33 through 41. The Reservoir Pressure (Pr) varies from orifice and also by regime. The Chamber Pressure Pc is set at .187 Pa for every experiment and is determined by the pump. Figure 33 is the mass flow rate versus time and the Knudsen number versus time. The flow rate is near constant for the entire time span and the Knudsen number is below .01 for the entire span. The Pr is equal to 6000 Pa for this case.

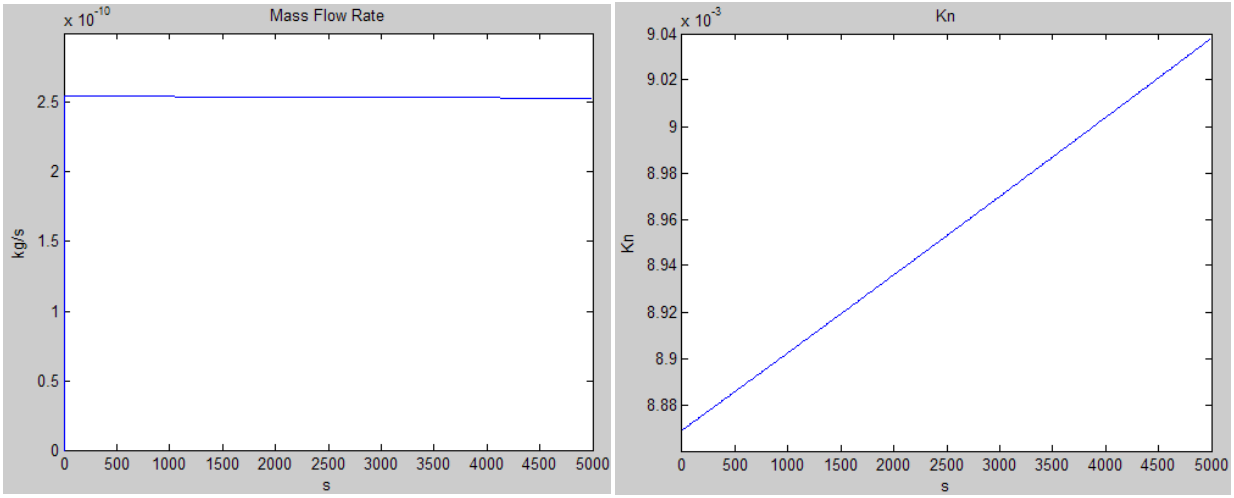

Figure 33 mass flow and Knudsen number versus time, for the 100 micron continuum flow

Figure 34 is Knudsen number and mass flow versus time for transitional flow; the Pr for this case is 3000 Pa.

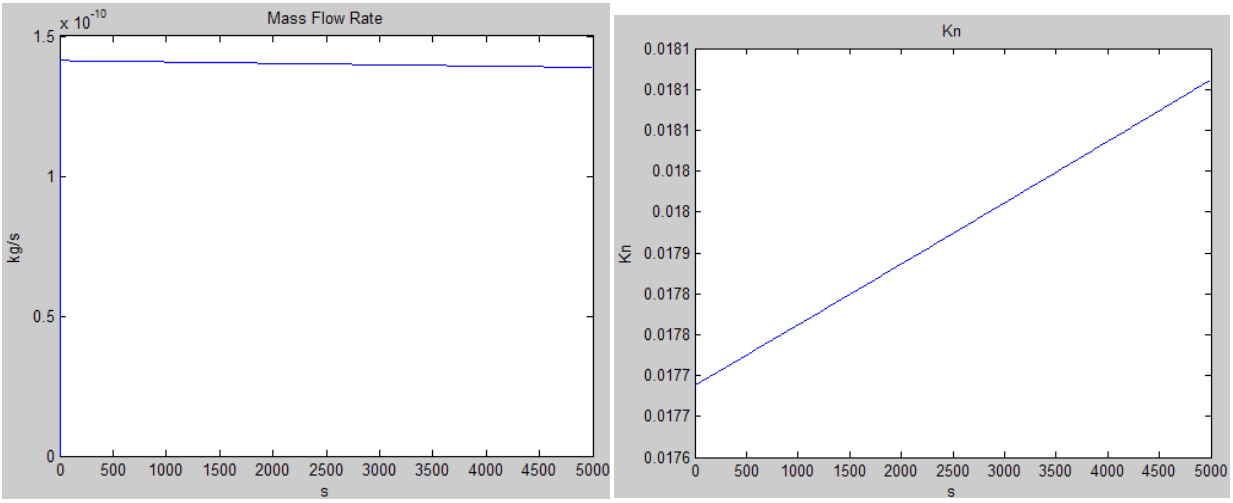

Figure 34 mass flow and Kn number for 100 micron tube transitional flow.

In figure 35, the mass flow and Kn number for free molecular flow are shown. These results predict, that the 100 micron orifice is a poor choice to run a stable experiment in the free molecular regime. This is due to the low pressure required to produce such a flow, less than 5.124 Pa, coupled with the rate at which pressure is lost, there is simply too small of a range. The initial Pr was set to 5 Pa.

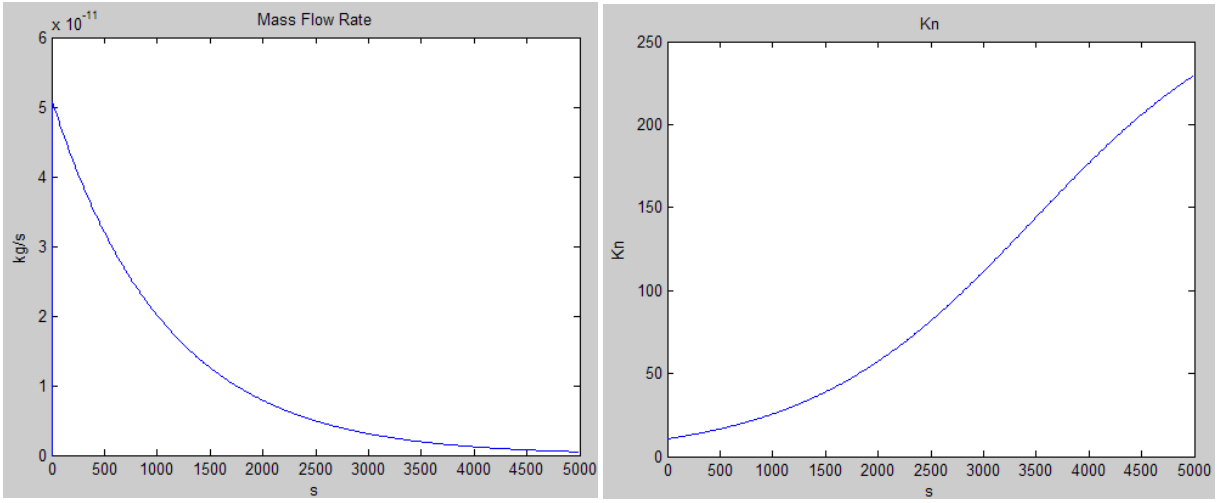

Figure 35 mass flow and Kn number for a 100 micron tube in free molecular flow

The next set of data is for the 10 micron tube. The pressure ranges for each regime are an order of magnitude greater than those for the 100 micron tube. Figure 36 shows the mass flow and Kn number for the 10 micron tube with a Pr of 60,000 Pa, resulting in continuum flow.

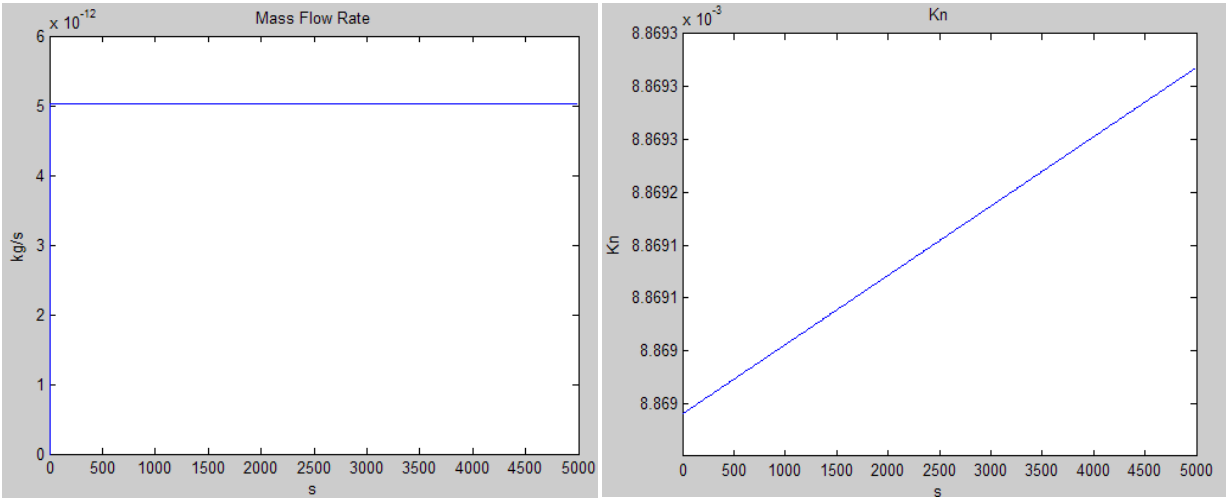

Figure 36 mass flow and Kn number for 10 micron tube, continuum flow

Figure 37 shows results for the 10 micron tube in transitional flow. Here, as in the continuum flow, the mass flow rate is much more stable over a longer period of time.

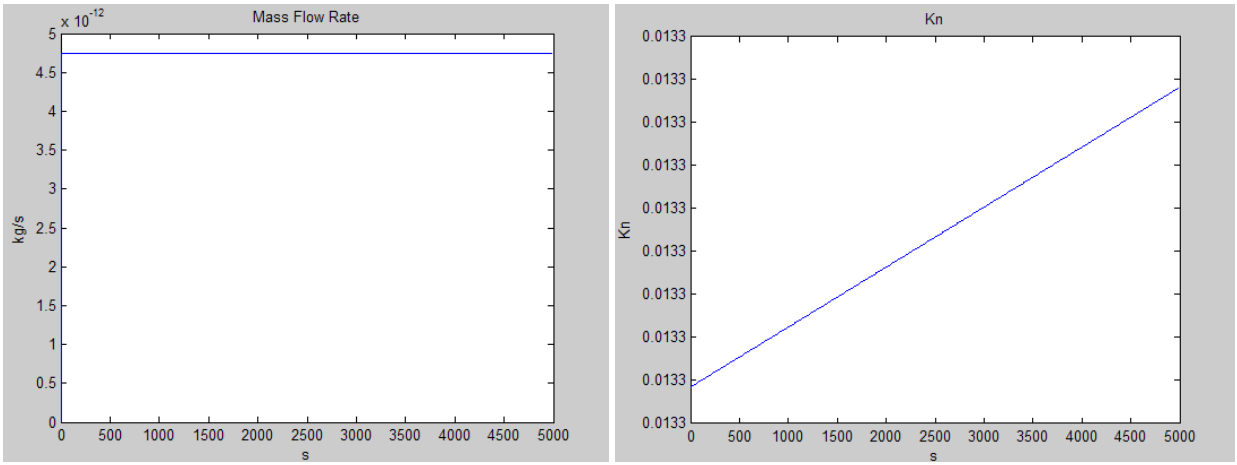

Figure 37 mass flow and Kn number for 10 micron tube, transitional flow

The free molecular regime is much more stable over time for the 10 micron tube than the 100 micron tube, but it still drops, significantly faster than the other regimes. Figure 38 displays the 10 micron tubes's free molecular regime.

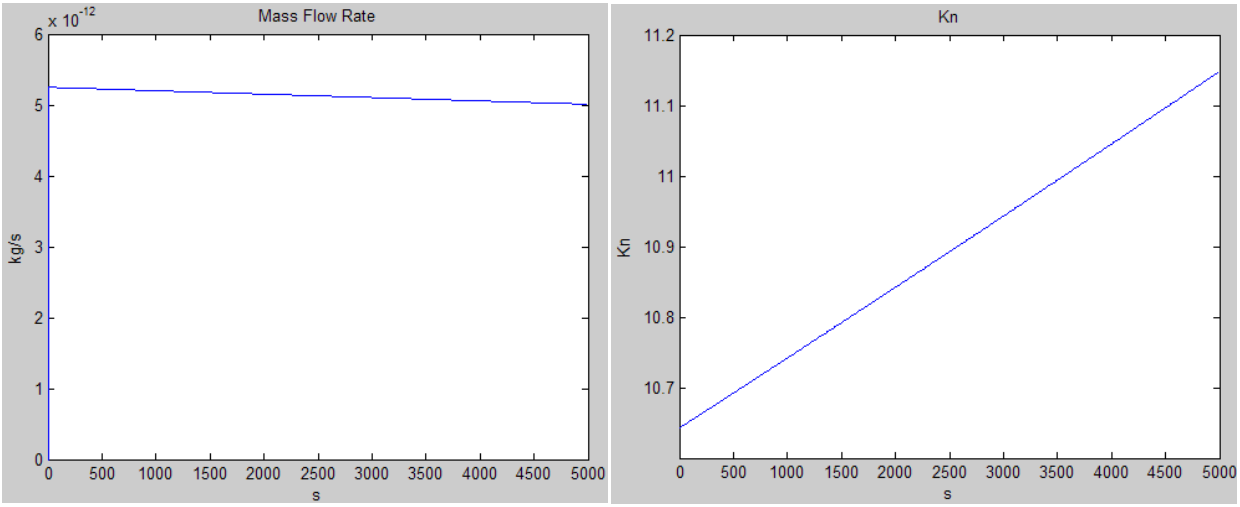

Figure 38 mass flow and Kn number for the 10 micron tube in free molecular flow

Unlike the 100 micron's free molecular results the 10 micron's is stable enough to perform an experiment over time.

The 1 micron tube, is unique in that it actually requires Pr values greater than atmospheric to achieve transitional and continuum flow. This also gives it the benefit of having

the greatest pressure range to escape rate ratio, making it ideal for long runs, it's mass flow rate is in the nano-scale though. Figure 39 show the continuum regime results for the 1 micron tube. For example a 1 micron hole between a vacuum and atmosphere would only produce transitional flow. The Pr used for the continuum case is 600000 Pa nearly 6 time atmospheric pressure.

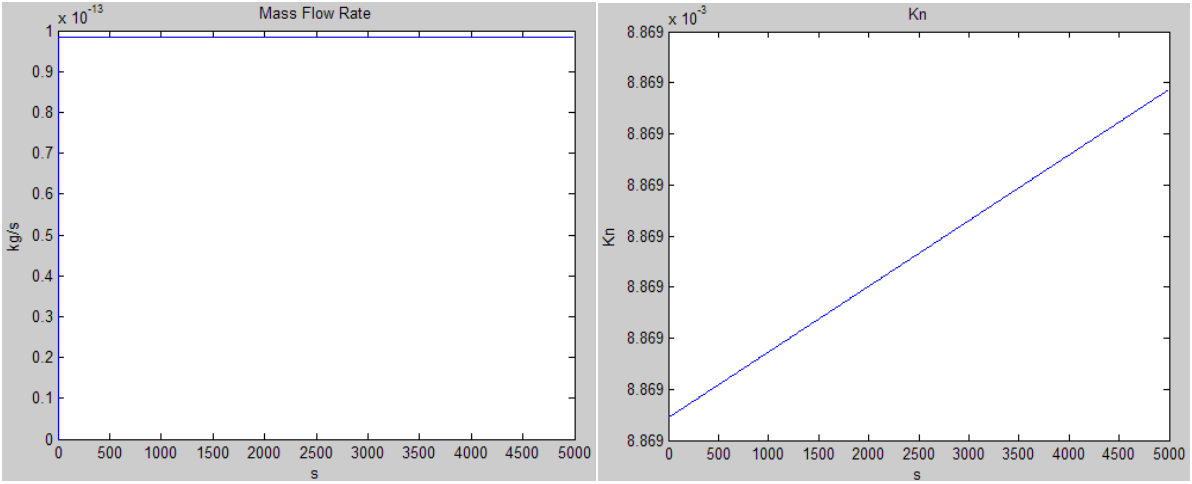

Figure 39 mass flow and Kn number for 1 micron, continuum flow

Transitional flow for the 1 micron hole has a very large range, but for consistency the 400000 Pa was chosen. Figure 40 show the results for transitional flow in a 1 micron tube.

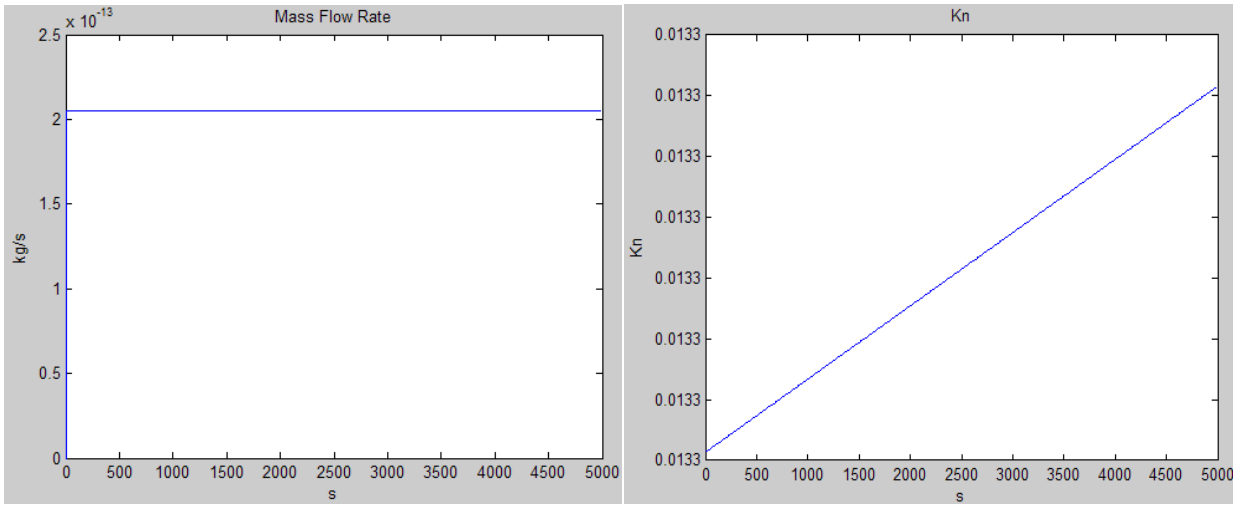

Figure 40 mass flow and Kn number for 1 micron, transitional flow

The 1 micron tube produces the most stable results for the free molecular regime; however, the low rate of pressure escape make using this size tube for anything but free molecular flow, may cause time complications if no other way to release excess pressure is

provided. Figure 41 show the results of the free molecular regime for the 1 micron tube. A Pr of 500 Pa was used for the initial Pressure.

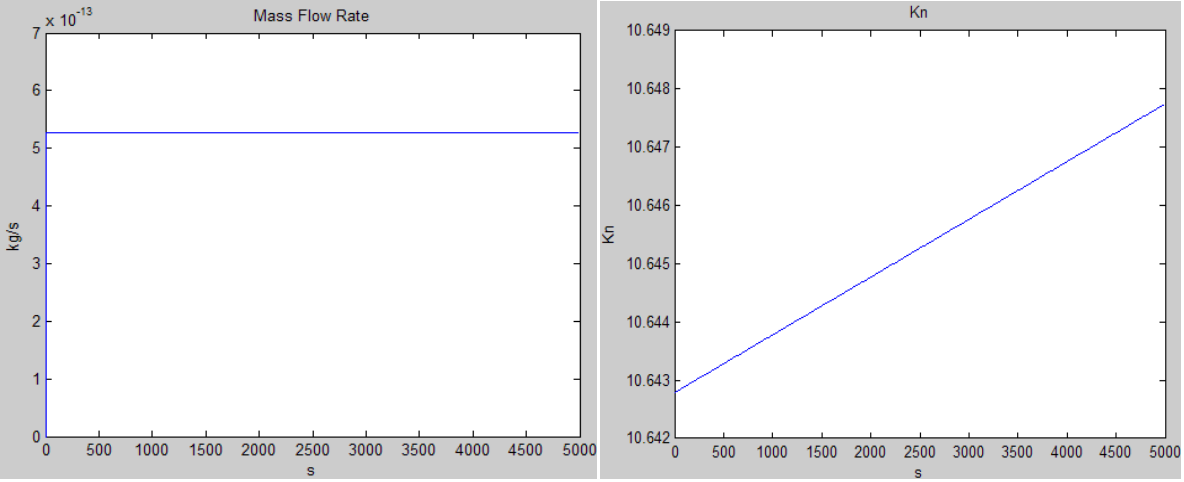

Figure 41 mass flow and Kn number for a 1 micron tube, free molecular regime

In summary, the 100 micron tube is good for large mass flow rates, it does have the drawback of having a large pressure escape rate. This could be alleviated with a device that regulated mass flow. The 10 micron tube is in the middle it has a lower escape rate and higher pressure ranges. This makes it an ideal candidate for pressure decay method or the mass flow controller. The 1 micron tube is the best tube for free molecular, and pressure decay is the only way to accurately measure its mass flow. This tube also has the most stable flow rate.

4.3 FLUENT Simulations

Several simulation runs were performed with FLUENT. These simulations were of flow through micro tubes with diameters equal to the nozzle diameter. Essentially these are very long nozzles. Multiple versions of each diameter were tested, one with a short length to diameter aspect ratio and one with a large aspect ratio. These simulations could only be run for continuum flow due to the restrictions of FLUENT. Because FLUENT uses the Navier-Stokes equations, it is unable to simulate rarefied flow accurately, it does allow for a wall slip velocity, but it requires additional information about the wall's construction. Pressure based inlets and outlets were applied to the ends of the pipe. Figure 35 shows a velocity vector field for the 100 micron tube with a inlet pressure (Pr) of 6000 Pa and an exit pressure (Pc) of .187 Pa. As the gas enters the

tube, the velocity goes from uniform to having a parabolic profile before leaving the tube. This demonstrated that the simulation is producing expected behavior at the small scale.

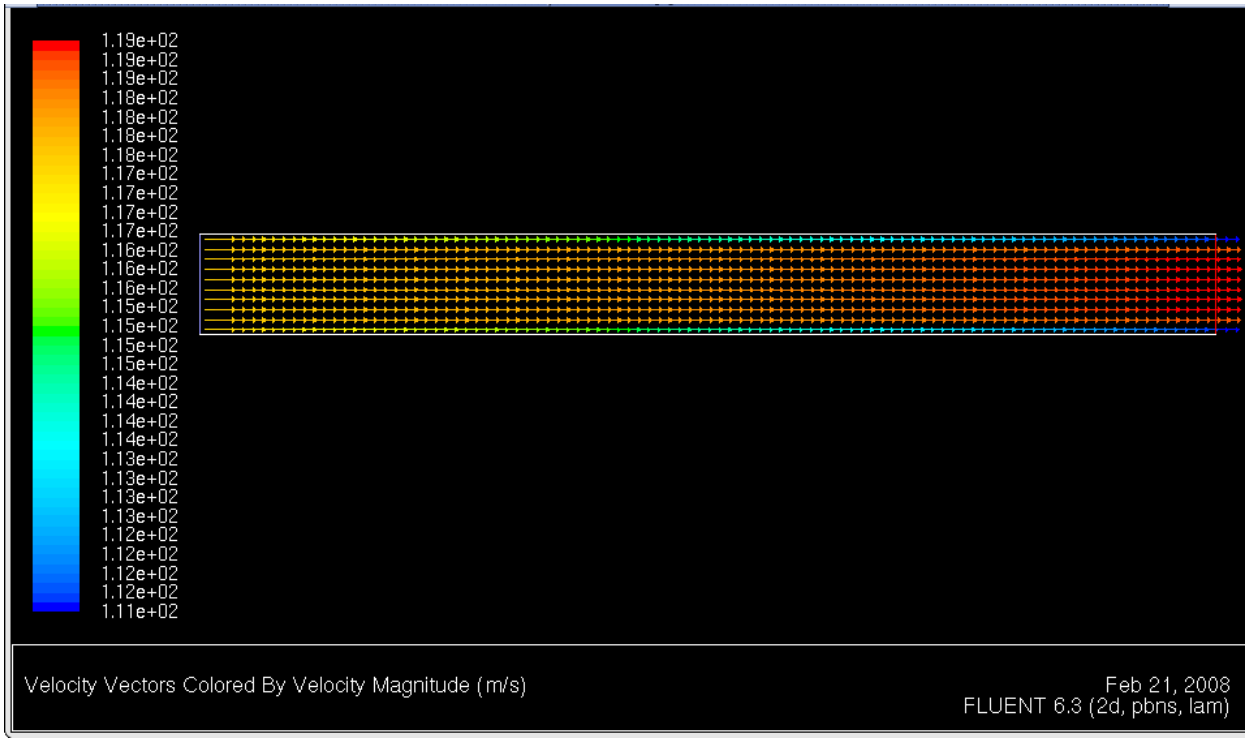

Figure 42 FLUENT Run for the 100 micron continuum flow (short tube)

Another set of simulations were run for the 10 micron tubes, one for the short tube and one for the longer tube. Figure 36 display the velocity magnitude by a color contour. Once again the boundary layer develops as the viscous effects take effect. The long tube is 10000 diameters long.

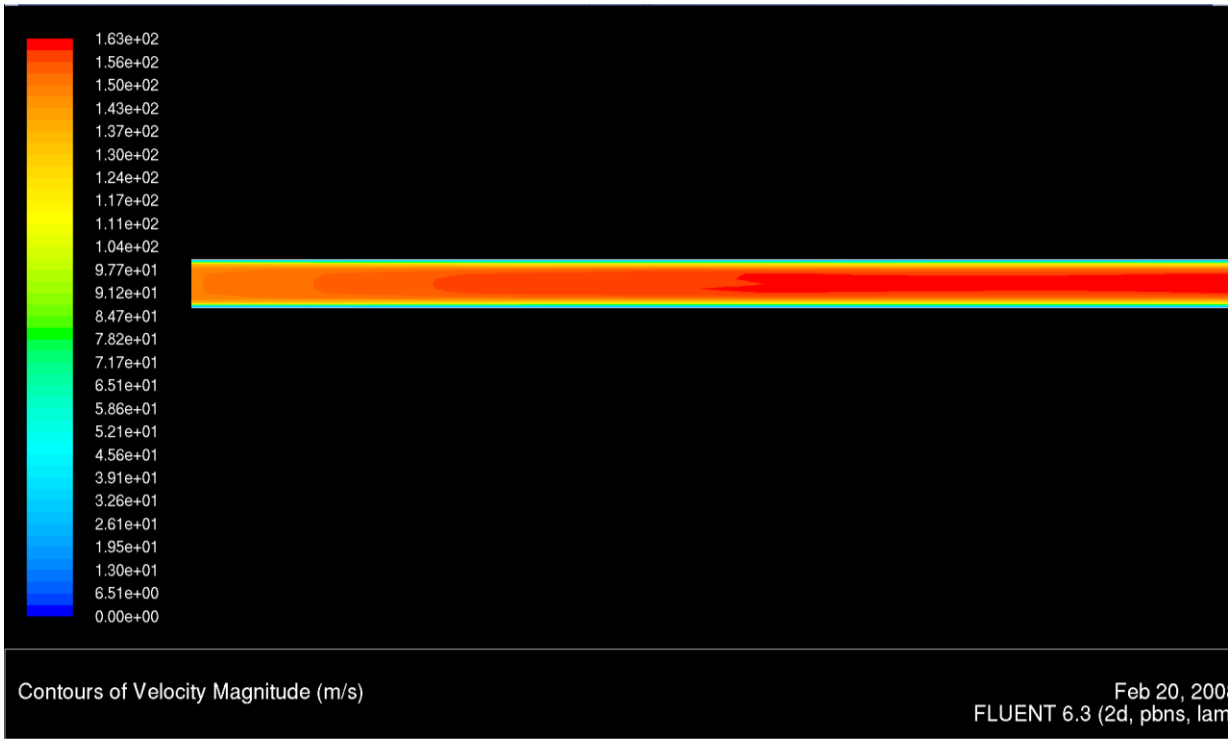

Figure 43 Velocity Contours for the 10 micron, longer tube

The flow displays a similar behavior in the short pipe except the speed is greater, this is most likely due to the shorter size tube producing less resistance to the flow. The short tube is 100 diameters long. Figure 37 show the velocity contours of the short tube.

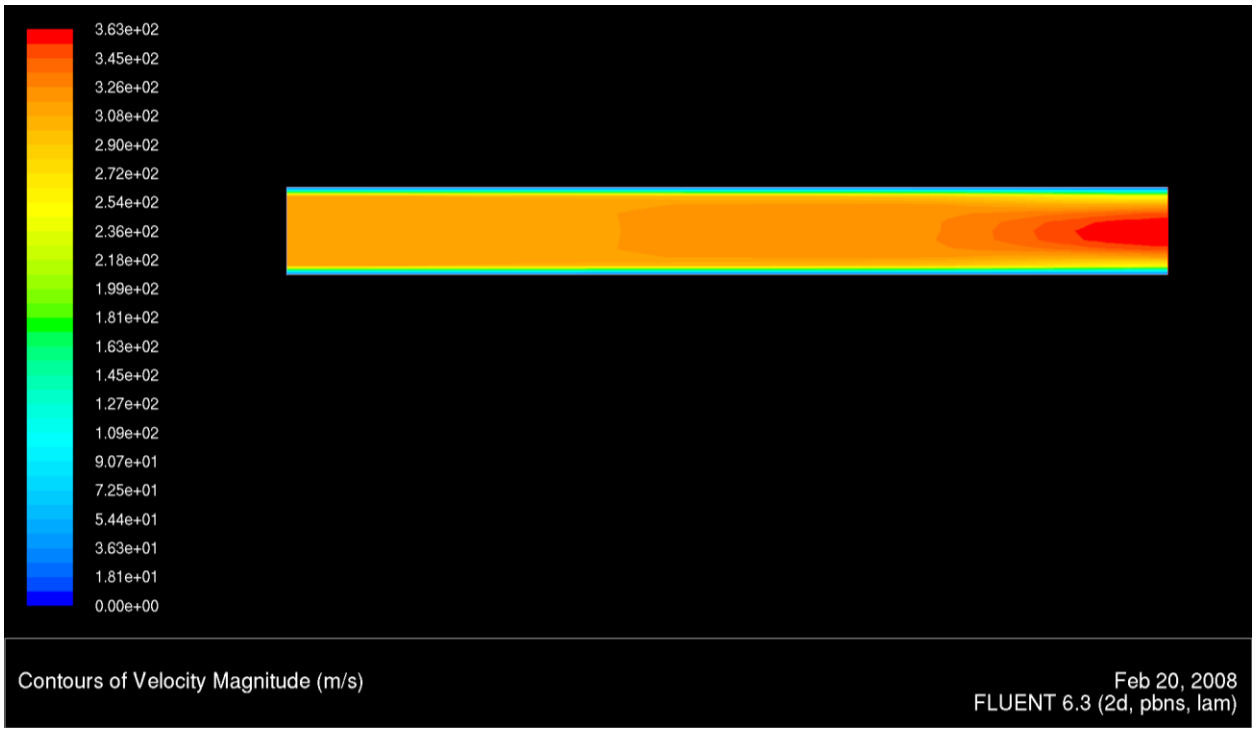

Figure 44 The 10 micron short tube velocity contours

5. Conclusions

5.1 A Support Structure

Through much iteration the design team came to its final design. Creating a table that would hold the load was not the difficult aspect of this challenge, creating a table which was light weight and cost effective was a much more difficult task. Through the use of fully boxed frame and a steel table top a working design was created. The hoisting mechanism was also a much greater challenge which consumed more time than was originally planned. Again many different approaches were taken. Most of the iterations used concepts for lifting mechanisms which are found in various industrial fields. Again weight and cost were the primary limitations for the device. The final lifting mechanism was integrated into the support system. Through the use of Pro Mechanic an analysis was run on both the table as well as the lifting system which insured the integrity of the design.

5.2 Table Top Deflection

The table surface that will hold the equipment was analyzed in Pro Mechanica. The deflection and weight were the design team's main concern. Originally the table top weighed too much. Once the table top was modeled at an acceptable weight there was an issue with deflection. To solve this issue the support structure beneath the table top was changed and a cross member was installed to help support the table top. The cross member effectively solved the deflection issue.

5.3 Overall Weight of System

The system was not to exceed 100 lbf-300 lbf. The reason for this requirement was to eliminate the possibility of overloading the concrete slab on the 3rd floor which would be supporting the system. Each step of the way through the design process weight was taken into consideration. Through the use of boxed frame members rather then sold members the strength of the support system was increased while the weight decreased. To increase the surface area which the weight would be distributed to the floor through boxed frame members were laid horizontally across the floor. Using this design rather than the standard table legs which create a very high point force enabled us to meet the design criteria of 100-300 lbf.

5.4 Fluid Mechanics

The data from the simulations made several issues clear. The 100 micron and 10 micron nozzles are good for continuum and transitional flows. The 1 micron is good for free molecular, but its driving pressures for transitional and continuum are high. Using various nozzles, mass flows that range from 10^{-10} to 10^{-13} kg/s. The FLUENT simulations predict that the flow at the very small scales should behave like its regime classification.

References

Arkilic, E.B.; Schmidt, M.A.; Breuer, K.S.; *Gaseous Slip Flow in Long Microchannels.*, Journal of Microelectomechanical Systems Volume 6 Issue 2 1997

Chamberlin, R. E., and Gatsonis, N. A., "Numerical Modeling of Gas Expansion From Microtubes," CNMM2006-96120, Proc. of the ASME 4th International Conference on Nanochannels, Microchannels and Minichannels, Limerick, Ireland, June 2006a.

Chamberlin, R. E., and Gatsonis, N. A., "DSMC Simulation of Microjet Expansion and the Design of a Micro Pitot Probe," AIAA- 2006 3799, 9th AIAA Joint Thermophysics and Heat Transfer Conference, San Francisco, CA, June 2006b.

FLUENT software packaere (educational edition)

Gravesen, Peter; Branebjerg, Jens; Jensen, Ole Sondergard. *Microfluidics A Review*, Journal of Micromechanics and Micro-engineering Volume 3 Number 4 1993

Heller, Jason; Padden, Tim. *A Microscale Mass-Flow Measuring System.* WPI MQP 2006

PTC Pro Engineer Wildfire 2.0 software package (educational edition)

Appendix A Matlab code

```
clear all
%Parameters
V=0.001;% Cubic meters
d=100*10^-6;%diameter of opening in meters
P1init=8000; %pascal
P2=10; %Pascals
T1=297.9;%Kelvin
T2=297.9;%Kelvin
Av=6.022*10^(-23);%Avogadro number
k=1.38*10^(-23);%Boltzmann constant
r=296.8;%specific gas constant for N2
pi=3.1415;
deltat=10;%seconds
m=46.5*10^(-27);%molecular mass of N2 in kg
dmol=4.17*10^(-10);%molecular diameter of N2 in meters
gamma=1.407; %specific heat ratio

%Calculations
n1(1)=P1init/(k*T1);%particles per cubic meter
N(1)=n1(1)*V;
n2=P2/(k*T2);
P1(1)=P1init;
t(1)=0;
lambda(1)=1/(sqrt(2)*pi*dmol^2*n1(1));
Kn(1)=lambda/d;
a1(1)=sqrt((gamma*P1(1))/(m*n1(1)));%the speeed of sound in reservoir 1

%calc method flag: flag:1-cont.,2-trans,3-FM
f(1)=0;

for i=2:1:500;
    if Kn(i-1)>=10;%kinetic effusion
        Nout(i)=(sqrt(k/(2*pi*m))*(n1(i-1)*sqrt(T1)-
n2*sqrt(T2)))*((pi*d^2)/4)*deltat;%net particles out
        f(i)=3;
    else if Kn(i-1)<=0.01;%continuum
            Nout(i)=n1(i-1)*a1(i-1)*(P2/P1(i-1))^(1/gamma)*(sqrt((2/(gamma-
1))*(1-(P2/P1(i-1))^((gamma-1)/gamma))))*((pi*d^2)/4)*deltat;%particle flux
            f(i)=1;
        else
            Nout(i)=((sqrt(k/(2*pi*m))*(n1(i-1)*sqrt(T1)-
n2*sqrt(T2)))*((pi*d^2)/4)*deltat)*(Kn(i-1)-0.01)/10+(n1(i-1)*a1(i-
1)*(P2/P1(i-1))^(1/gamma)*(sqrt((2/(gamma-1))*(1-(P2/P1(i-1))^((gamma-
1)/gamma))))*((pi*d^2)/4)*deltat)*(0.01/Kn(i-1));%transition
            f(i)=2;
        end
    end
    N(i)=N(i-1)-Nout(i);
    n1(i)=N(i)/V;
    P1(i)=n1(i)*k*T1;
    mdotexp(i)=((m*V)/(k*T1))*((P1(i-1)-P1(i))/deltat);%mass flux during
experiment
    a1(i)=sqrt(gamma*P1(i)/(m*n1(i)));%the speed of sound in reservoir 1
```

```
    t(i)=t(i-1)+deltat;
    lambda(i)=1/(sqrt(2)*pi*dmol^2*n1(i));
    Kn(i)=lambda(i)/d;
end
Kn(1)
mdotexp(2)
length(t);
length(P1);

figure(1)
subplot(2,2,1); plot(t,P1)
title('P')
xlabel('s')
ylabel('Pa')
subplot(2,2,2); plot(t,Kn)
title('Kn')
xlabel('s')
ylabel('Kn')
subplot(2,2,3); plot(t,f)
title('Calculation Method')
xlabel('s')
ylabel('f')
subplot(2,2,4); plot(t,mdotexp)
title('Mass Flow Rate')
xlabel('s')
ylabel('kg/s')
figure(2)
plot(t,Kn)
title('Kn')
xlabel('s')
ylabel('Kn')
figure(3)
plot(t,f)
title('f')
xlabel('s')
ylabel('f')
figure(4)
plot(t,mdotexp)
title('Mass Flow Rate')
xlabel('s')
ylabel('kg/s')
figure(5)
plot(P1,mdotexp)
title('mdot Vs P')
xlabel('Pa')
ylabel('kg/s')
figure(6)
plot(P1,Kn)
title('Kn Vs P1')
xlabel('Pa')
ylabel('Kn')
%subplot(3,1,1),plot(t,P1),grid,title('P'),xlabel('s'),ylabel('Pa');
%subplot(3,1,2),plot(t,Kn),grid,title('Kn'),xlabel('s'),ylabel('Kn');
%subplot(3,1,3),plot(t,f),title('Calc. Method'),xlabel('s'),ylabel('f');
%subplot(3,1,3),plot(P1,mdotexp),title('mdotexp Vs
P'),xlabel('Pa'),ylabel('kg/s');
%subplot (3,1,3),plot (P1,Kn),title('Kn Vs P1'),xlabel('Pa'),ylabel('Kn');
```

```
%subplot(3,1,1),plot(t,P1),grid,title('P'),xlabel('s'),ylabel('Pa');
%subplot(3,1,2),plot(t,mdotexp),grid,title('Mass Flow
%('Rate'),xlabel('s'),ylabel('kg/s');
%subplot(3,1,3),plot(t,Kn),grid,title('Kn'),xlabel('s'),ylabel('Kn');
%plot(t,Kn),grid,title('Kn'),xlabel('s'),ylabel('Kn');
%x=flipud(rot90(P1));
%y=flipud(rot90(mdotexp));
%z=flipud(rot90(t));
%xlswrite('pressure_transducer_tests.xls',y,'Sheet1','G2');
%xlswrite('pressure_transducer_tests.xls',z,'Sheet1','H2');
%xlswrite('pressure_transducer_tests.xls',x,'Sheet1','I2');
```

Appendix B

PRINCIPAL STRESSES

In an elastic body that is subject to a three-dimensional system of loads, a system of stresses is developed. These are called the normal (σ) and shear (τ) stresses. For a two-dimensional plane:

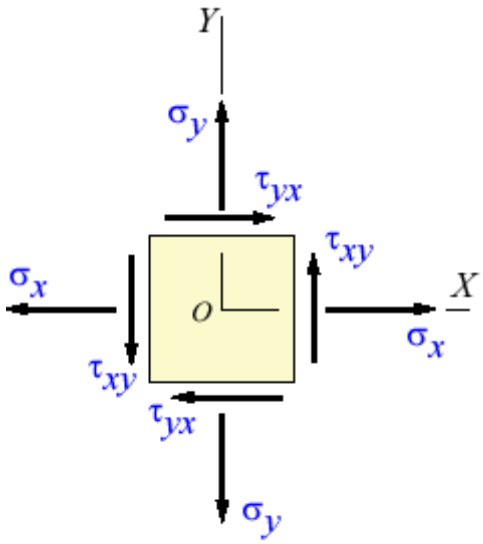

Stresses in given coordinate system

In certain cases, the directions of the stresses (x',y',z') do not line up with the original coordinate set (x,y,z):

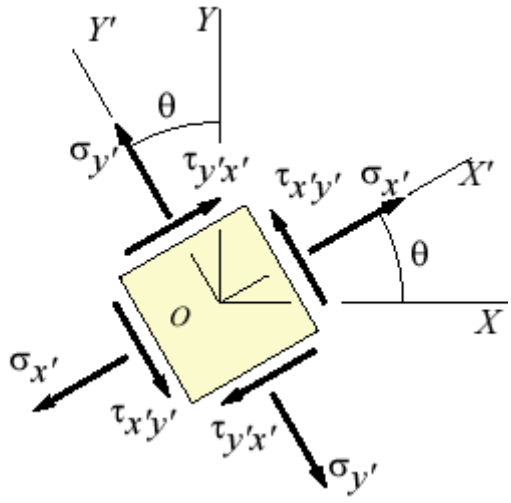

In this case the transformation can be obtained with the following equations:

$$\sigma_{x'} = \frac{\sigma_x + \sigma_y}{2} + \frac{\sigma_x - \sigma_y}{2}\cos 2\theta + \tau_{xy}\sin 2\theta$$
$$\sigma_{y'} = \frac{\sigma_x + \sigma_y}{2} - \frac{\sigma_x - \sigma_y}{2}\cos 2\theta - \tau_{xy}\sin 2\theta$$
$$= \sigma_x + \sigma_y - \sigma_{x'}$$
$$\tau_{x'y'} = -\frac{\sigma_x - \sigma_y}{2}\sin 2\theta + \tau_{xy}\cos 2\theta$$

There is an angle where the stresses are only normal stresses. These stresses are the principal stresses and are found from the original stresses in the x, y, and z directions. For a two-dimensional plane:

$$\sigma_{1,2} = \frac{\sigma_x + \sigma_y}{2} \pm \sqrt{\left(\frac{\sigma_x - \sigma_y}{2}\right)^2 + {\tau_{xy}}^2}$$

The variable σ_1 is commonly known as the max prin. stress, and σ_2 is commonly known as the min, prin stress.

VON MISES CRITERION

The Von Misses Criterion, also known as the maximum distortion energy criterion is often used to estimate the yield stress of ductile materials. On a plane stress, the Von Misses stress (σ_y) reduces to:

$${\sigma_1}^2 - \sigma_1\sigma_2 + {\sigma_2}^2 \leq {\sigma_y}^2$$

This equation represents a principal stress ellipse shown below:

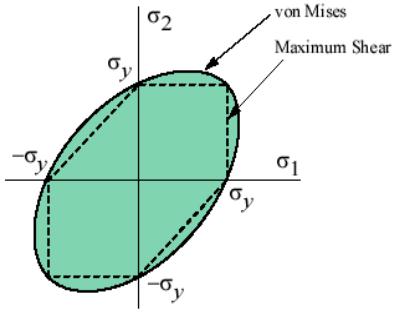
σ2
von Mises
Maximum Shear
σy
−σy
σ1
σy
−σy